Effect of Reduced System Inertia Due to Increased Renewable Resource Penetration on Power System Stability

by

Iknoor Singh

A Thesis Presented in Partial Fulfillment
of the Requirements for the Degree
Master of Science

Approved June 2012 by the
Graduate Supervisory Committee:

Vijay Vittal, Chair
Raja Ayyanar
Kory Hedman

ARIZONA STATE UNIVERSITY

August 2012

ABSTRACT

This thesis concerns with the impact of renewable generation resources on the power system stability. The rapidly increasing integration of renewable energy sources into the grid can change the way power systems operate and respond to system disturbances. This is because the available inertia from synchronous machines, which helps in damping system oscillations, gets reduced as an increase in renewables like wind and solar photovoltaics is accompanied by a decrease in conventional generators. This aspect of high penetration of renewables has the potential to affect the rotor angle stability and small signal stability of power systems.

The system with increased renewables is mathematically modeled to represent wind and solar resources. Transient and small signal stability studies are performed for various operating cases. The main conclusion drawn from the different studies is that increased renewable penetration causes a few instability problems, most of which are either localized and do not adversely affect the overall system stability. It is also found that the critical inter-area modes of oscillations are sufficiently damped.

ACKNOWLEDGEMENTS

I would like to first and foremost offer my sincerest gratitude to my advisor, Dr. Vijay Vittal, whose encouragement, guidance and support from the initial to the final level enabled me to develop an understanding of the subject. I attribute the level of my Master's degree to his encouragement and effort and without him this thesis, too would not have been completed. One simply could not wish for a friendlier supervisor. I also want to express my gratitude to Dr. Raja Ayyanar and Dr. Kory Hedman for their time and consideration in being a part of my graduate supervisory committee.

I especially want to thank my parents Mr. Sukhdayal Singh and Mrs. Devender Kaur for the continual inspiration and motivation to pursue my utmost goals. I also would like to thank my friends and roommates who stood beside me and encouraged me constantly.

TABLE OF CONTENTS

CHAPTER Page

CHAPTER Page

LIST OF TABLES

Table Page

LIST OF FIGURES

Figure Page

Figure Page

NOMENCLATURE

A	State or plant matrix
A_r	Area swept by rotor blades
B	Control or input matrix
bf	Bus fault
C	Output matrix
CST	Central Solar Thermal
C_p	Wind power coefficient
D	Feed forward matrix
DFIG	Doubly Fed Induction Generator
E''_{qcmd}	Voltage command
f	Frequency of oscillation
FCWTG	Full Converter Wind Turbine
FSIG	Fixed-Speed Induction Generator
g	Matrix of non-linear functions
GE	General Electric
I_{Pcmd}	Real current command signal
n	Order of system
P	Mechanical power extracted from wind
P_e	Power output of generator

P_{gen}	Plant output specified in the power flow case considered
P_{import}	Power being imported in the study area
p_{ki}	Participation factor of the k^{th} state variable in the i^{th} mode
P_{max}	Maximum output rating of each unit
P_r	Power delivered to the rotor
P_s	Power delivered by the stator
PI	Proportional Integral Control
POI	Point of Interconnection
PSLF	Positive Sequence Load Flow
PSS	Power System Stabilizer
PV	Photovoltaics
Q_{cmd}	Reactive power control block output signal
r	Number of inputs
RPS	Renewable Portfolio Standards
s	Slip
SSAT	Small Signal Analysis Tool
SVC	Static VAR Compensator
u	Input matrix
V_{ref}	Reference voltage
v_ω	Wind speed
WTG	Wind Turbine Generator

x	State variable matrix
y	Output matrix
α	Real part of eigenvalue
β	Imaginary part of eigenvalue
ξ	Damping ratio
θ	Blade pitch angle
λ	Eigenvalue
ρ	Air density
ϕ	Right eigenvector
ψ	Left eigenvector
μ	Ratio of rotor blade tip speed to wind speed
ω_{ref}	Reference speed

Chapter 1. INTRODUCTION TO CHALLENGES POSED BY RENEWABLES

1.1 Introduction

Due to the greater need to meet various renewable portfolio standards to increase renewable resource generation to reduce the green-house emissions and because of an abundance of wind and solar energy resources in the U.S., renewable power generation integration has been increasing at an unprecedented pace. The average wind energy growth rate in the U.S. is about 25% per annum for the past five years with predictions for even higher rates for next few decades [1],[2]. Similarly, generation from solar photovoltaics (PV) and solar thermal resources have also increased by more than 35% per annum for the last two years [2]. But with the transmission grid throughout the nation already loaded close to its limits, the delivery of electric power from these renewable resources to the load centers becomes a challenging task.

With many states adopting their respective renewable portfolio standards (RPS) to accomplish the ambitious renewable energy targets in next 10-15 years, integrating these renewables into the power system poses great technical challenges. One of the challenges is to ensure the transient and small-signal stability of the power system. A bulk of the new renewable capacity addition will come from wind generators, solar PVs and centralized solar thermal plants (CST). The introduction of new renewable resources together with the phasing out of conventional fossil-fired power plants has the potential of drastically changing the way

power systems work in terms of change in power flow patterns, effect on synchronizing powers and the sensitivity of the system to faults. While the effect of conventional synchronous generators on system stability is well understood, it is not the case for wind and solar power plants. Their intermittent, non-dispatchable nature puts them at a disadvantage from the system reliability point of view. Also, because of their inherently different operating principles than synchronous machines, their interaction with the power system is also markedly different. The problem becomes even more uncertain at high renewable penetration levels as has been envisioned in the RPS standards. Most of the modern wind generators are connected to the grid through a power electronics interface thereby effectively masking their rotating mass inertia. Hence, there is no inertia available from these wind generators to dampen the electromechanical oscillations due to power system faults. This is also true for solar PV farms. Therefore, high levels of wind and solar PV penetrations, together with replacement of conventional fossil-fired power plants cause an appreciable decrease in overall system inertia. Hence, it is necessary to correctly model these renewable resources and conduct a comprehensive system study to examine the transient and small-signal stability of the system with the new resources included.

As compared to conventional synchronous generators, wind and solar photovoltaic (PV) generation resources show markedly different characteristics at the point of interconnection (POI) with the bulk power system. The recent advances in wind generation technologies have led to the development of variable speed

wind turbine generators and these generators are expected to form the bulk of new wind generation installations throughout the world.

1.2 Problem statement and rationale

The increased penetration of renewable energy resources with power electronics converters shows marked impact on system stability. Following a large disturbance, the restoring forces that bring the position of the affected generators back to nominal values are related to the interaction between the synchronizing forces and the total system inertia. In the case of power electronics based renewable resources; however, the electrical power generated by the unit is effectively tightly controlled by the current control loops of the converter. Subsequent to an electrical disturbance, the converter quickly controls the unit to return to its pre-disturbance power output, thereby curtailing the potential inertial response of the turbine from the grid. Hence, with increased penetration of such generation resources, the effective inertia of the system is markedly reduced, thereby, potentially affecting the system dynamic performance.

The reduced inertia affects the system in two ways: (i) after a disturbance the effective angular acceleration of the rotors of synchronous generators would be increased. Consequently, the restoring synchronizing forces would have to be larger to bring the disturbed machines back to equilibrium position, and (ii) the rate of decay of frequency would be increased for generation loss events and therefore, the transient stability of the system could be compromised for certain severe disturbances.

The converter controls the rotor speed and electrical power, thereby decoupling the turbine from the grid. It also damps out any rotor speed oscillations that may occur within the wind turbine generator (WTG). WTGs primarily only have four mechanisms by which they can affect the damping of electromechanical modes (since they themselves do not participate in the modes) [11]:

1. Displacing synchronous machines thereby affecting the modes
2. Impacting major path flows thereby affecting the synchronizing forces
3. Displacing synchronous machines that have power system stabilizers
4. DFIG controls interacting with the damping torque on nearby large synchronous generators

The changes in operations of the grid due to the placement of wind farms can also impact the oscillations. Wind farms are normally located far from major load centers. This requires power delivery over longer distances and might cause overloading of already congested lines. The same is true for solar generation at commercial scales. This scenario might lead to significant change in generation profile and power flow, thereby, affecting the small signal stability of the system. Given this scenario, the major part of the present work encompasses the issues related to system dynamic performance with the penetration of wind farms and solar generation facilities. The impact study is carried out by perturbing the system with three-phase short circuit faults and applying disturbances at various locations in the system.

The inertia constants of conventional synchronous generators of a large power plant are in the order of 2-9 s [3] and this inertia is automatically available as the frequency of the grid tends to decrease following a disturbance or loss of generation/transmission line. In the case of wind farms, as discussed above, the inertia of the turbine is effectively decoupled from the system. The decoupling of the inertia in wind farms, however, can be overcome by appropriate use of control. Significant amount of kinetic energy is stored in the rotating turbine blades with typical inertia constants in the range of 2-6 s [4]. It is possible to exploit the isolated inertia and support the system if proper control mechanisms are developed.

1.3 Objectives

The overall objective of this research is to study the impact of increased penetration of renewable resources on transient and small signal stability of the bulk power system. The steps to achieve this objective are as follows:

- To develop a suitable model of the system and incorporate wind, solar PV and solar thermal renewable generation resources that would have an impact on the system performance
- To identify critical contingencies which could affect the system by conducting *N-1* and *N-2* static security analyses
- Based on the highly ranked static contingencies, perform transient stability studies within the system and at the boundary with neighboring systems

- To examine if there is any detrimental impact on the system due to increased renewable penetration
- To conduct small signal stability analysis within the system and at the boundary with neighboring systems
- To provide a reasoning for the research findings

1.4 Organization of thesis

The thesis is organized in seven chapters. Chapter 1 gives an introduction which presents the background of the study. The chapter contains the problem statement, rationale and objectives of the study.

Chapter 2 presents the literature review with regard to several wind and solar power technologies in existence. The chapter also summarizes various research work carried out in the past in modeling of these technologies and their impact on power system operations and stability.

Chapter 3 deals with theory of mathematical modeling and control of various commercially available wind and solar power technologies so that they can be used for system stability studies. The fundamentals of transient and small signal stability studies of a power system are also discussed.

Chapter 4 provides the proposed methodology to carry out the study.

Chapter 5 gives the simulation results obtained and the inferences are drawn out of those results.

Chapter 6 concludes the findings from the work and proposes future work.

Chapter 2. LITERATURE REVIEW

DFIGs have the characteristics of independent control of reactive power from real power, and shorter response time of power electronic converters. Variable speed design of DFIG helps in limiting transient oscillations after a disturbance, leading to better rotor angle stability than a conventional synchronous generator. Modern DFIG based wind power plants with power electronics converters and low-voltage ride-through capability have been shown to provide stable operation even when connected to weak power grids [5]. A comparison between the conventional fixed speed wind turbines and the recent doubly-fed induction machines is provided in [6] where the operation of these two kinds of machines is compared during transient disturbances like three-phase faults, and network voltage sags. It is shown that whereas the inherent speed and power factor controls within the DFIGs help in improving the system stability and voltage recovery, the limitations of the fixed capacitor power factor correction in a fixed speed induction generator (FSIG) may lead to uncontrolled acceleration of the generator rotor. The instability problem in FSIG becomes more acute when the wind farm is connected to weak grid. As pointed out in [7] the DFIGs have a tendency to increase the inter-area oscillation damping by properly adjusting control parameters. It is shown that if the DFIG is operating under power factor control mode, the electromechanical eigenvalue damping increases with more wind power penetration. Even when the DFIG is operating in voltage control mode, the system does not show small signal stability problems provided there is proper tuning of reactive

power controllers. Further investigation of the effect of increased wind power penetration on small signal stability is investigated in [8] where it is pointed out that increase in wind power penetration can lead to either increase or decrease in inter-area oscillation damping depending upon the operating conditions. It is also pointed out that although wind generators as such do not deteriorate the inter area oscillations, the stability may still be affected due to the change in operational structures of the system such as significant changes in generation profiles and the power flow patterns over the lines as more and more wind power gets transmitted over longer distances. One particular scenario is discussed where the decrease in damping is caused due to the congestion of the lines in an already weak transmission system. It is also noted that if the damping decreases in a system, suitable power system stabilizers need to be installed. The effectiveness of suitably tuned PSS installed in the wind power generators in damping the electromechanical oscillations is further discussed in [9]. It is also noted that the PSS in wind generators should be tuned in coordination with those installed in synchronous generators for good damping throughout the bulk power system. A PSS has been proposed in [10] based upon flux magnitude-angle controller scheme. In this scheme, the magnitude of the rotor voltage vector and its phase angle are adjusted independently of each other to control the terminal voltage and electrical power respectively. This scheme is different from that of the excitation control of a synchronous machine, since the excitation control of a synchronous machine can change only the magnitude of the rotor flux vector and not its angle which coin-

cides with the physical position of the rotor itself. But a DFIG with the proposed scheme can adjust both the magnitude as well as position of the rotor flux vector, providing a much greater control capability. This scheme is shown to provide enhanced network damping over the full operating slip range covering both the sub-synchronous and super-synchronous operating regions. Also, the increased damping can be achieved without compromising the voltage control quality. This aspect is very different from a synchronous machine where damping improvement is accompanied by reduced voltage control performance. Further analysis on the impact of increased penetration of wind generators is examined in [11] where analysis method involves the conversion of DFIGs to equivalent MVA rating conventional round rotor synchronous machines. These machines are then evaluated for the sensitivity of eigenvalues with respect to inertia. The increase wind penetration is shown to have both positive and negative impacts upon the system stability depending upon different scenarios. The negative damping cases as identified in the eigenvalue analysis are also verified in the transient stability analysis by placing three phase faults close to the generators having the largest participation factors in the oscillatory modes. The same authors propose a PSS control mechanism [12] where the wind generator power output is fed as input to the PSS and this active power input command is modulated in phase opposition to the undamped power system oscillations. There is an additional control block with the terminal voltage as input to the PSS to be fed to the reactive power control loop. It is shown that such PSS design improves the damping of critical modes as seen in

eigenvalue analysis and also damps the low frequency inter area oscillation modes. Further simulation studies on high wind power penetration reveals that the transient stability worsens if faults are applied close to the wind farms [13]. This happens because of the crowbar operation at individual wind generators which causes significant reduction in active power generation as well as high absorption of reactive power. The studies also reveal that faults close to synchronous machines do not worsen transient stability because the power flows from wind generators help in maintaining synchronizing forces in the power system. To improve transient stability, avoidance of crowbar protection and deployment of active fault ride-through schemes are advocated. The impact of integrating large grid-level solar photovoltaic plants has also been investigated. It has been shown that solar PV plants if operated under constant voltage mode can help in improving system transient stability by increasing the loadability margin at which the system shows oscillatory behavior [14], which need not be true under constant reactive power mode of operation. It is pointed out that high solar PV penetration can either increase or decrease the damping of inter-area oscillation modes depending upon the location and penetration levels [15]. The solar PV generation also has the effect of changing the mode shape of the inter-area mode for the conventional synchronous generators which are not displaced by the PV generators. It is also noted that in the absence of sufficient damping due to increased PV generation, some synchronous generators in critical areas should be kept in service and not displaced by PV generators. Also, if the synchronous generators are absolutely nec-

essary to be displaced, then suitable measures like SVCs need to be installed to maintain sufficient damping of low frequency oscillations. The above mentioned finding is also asserted in [16] where it is stated that damping can either increase or decrease depending upon the solar PV penetration level. It is pointed out that for a fixed load; penetration beyond a critical operating condition decreases the damping of power system oscillations. Also, for a fixed solar PV generation, damping decreases with decrease in generation from conventional generators. Further studies, for example on IEEE-39 bus test bed [17], also confirm the fact that increasing solar PV penetration levels make the power system angle and voltage unstable in terms of more time to return to normal state on occurrence of a fault.

Chapter 3. THEORY AND MODELING OF RENEWABLES

3.1 Theory of renewables

3.1.1 Fixed speed wind turbine generator

The most basic wind generator uses fixed speed technology with squirrel cage induction generators. The generators using this technology are also referred as Type-1 wind generators in literature [18]. The generator is coupled to the grid through a connecting transformer. Since induction machines do not provide any reactive power output, power factor correction capacitors are usually provided at each wind turbine, which are typically rated around 30% of the wind generator capacity [6]. Figure 3.1 shows the schematic diagram of such a machine.

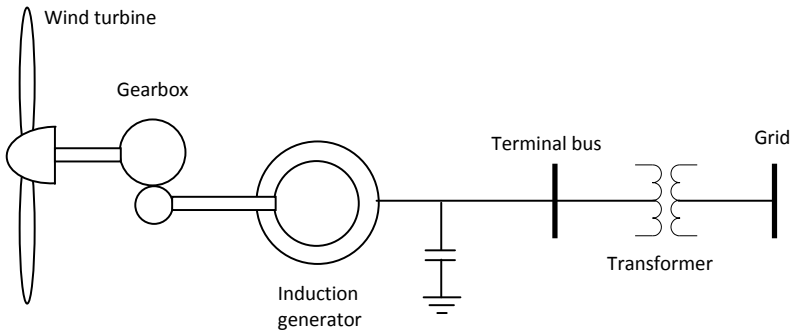

Figure 3.1 Fixed speed wind turbine generator

3.1.2 Variable speed wind turbine generator

The motivation for variable speed technology is the ability to capture greater wind energy. This concept allows operating the wind turbine at the optimum tip-speed ratio and hence at the optimum power coefficient for a wide wind speed range. The variable speed configuration is very flexible, in that it can be used to control different parameters, namely, active and reactive power, torque,

power factor or terminal voltage. The variable speed WTGs can act as a reactive power source or supply in contrast to a fixed speed generator which always absorbs reactive power. The two most widely used variable speed wind generator concepts are the DFIG and the full converter wind turbine (FCWTG).

Doubly fed induction generator wind turbine (Type-3)

The DFIG is basically a wound rotor induction generator using slip rings to take current into or out of the rotor. The rotor is fed through a voltage source converter and is operated at a variable ac frequency, thereby allowing for control of mechanical speed of the machine. The stator winding is coupled directly to the grid and the rotor winding is connected to a power converter as shown in Figure 3.2.

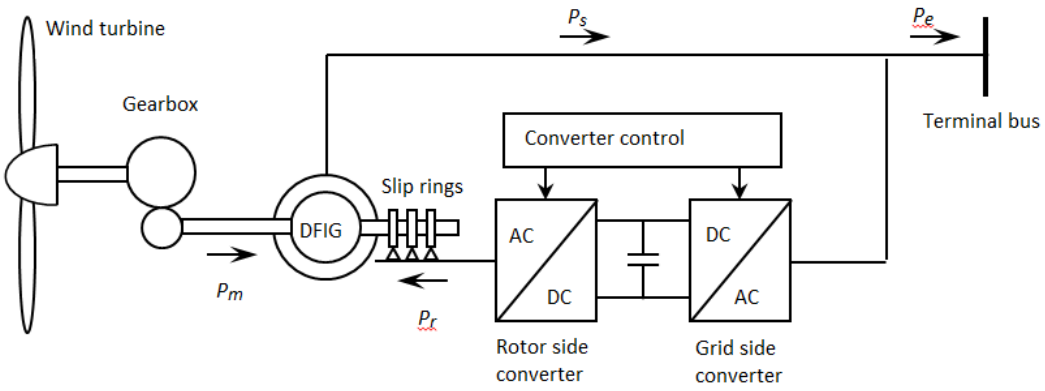

Figure 3.2 Doubly fed induction generator wind turbine (Type-3)

In a DFIG, the net power out of the machine is a combination of the power coming out of a machine's stator and that from the rotor (through converter) into the system. When the unit is operating at super-synchronous speeds real power is injected from the rotor, through the converter, into the system. When the unit is

operating at sub-synchronous speeds real power is absorbed from the system, through the converter, by the rotor [19]. At synchronous speeds, the voltage on the rotor is essentially dc and there is no significant net power interchange between the rotor and the system. Hence, the rotational speed of the DFIG determines whether the power is delivered to the grid through the stator only or through the stator and rotor [6]. The power delivered by the rotor and stator is given by [20],

$$P_r = sP_s \tag{3.1}$$

$$P_e = (1 \pm s)P_s \tag{3.2}$$

where P_e is the electrical power output of the generator, P_s is the power delivered by the stator and P_r is the power delivered to the rotor.

Full converter wind turbine generator (Type-4)

This design uses a conventional synchronous generator with a dc field or a permanent magnet to provide excitation. The advantage of this category of wind machines is the gearless design, since the generator is directly connected to the turbine and rotates at the same speed as that of turbine [19]. The generator is connected to the network through a back-to-back frequency converter, which completely decouples the generator from the network. Through this converter, the electrical output of the generator can be converted to system frequency over a wide range of electrical frequencies of the generator, enabling the machine operation over a wide range of speeds. The schematic of the converter driven synchronous generator based wind turbine is as shown in Figure 3.3.

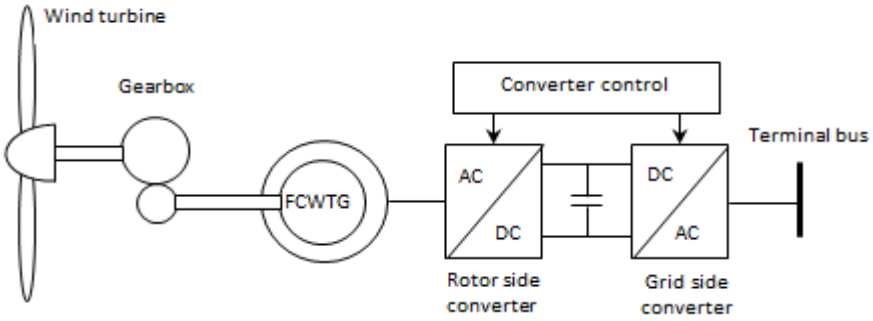

Figure 3.3 Full converter wind turbine generator

3.1.3 Solar PV generator

Since a solar PV generator's output is fed to the grid through a converter, it can be modeled similar to a FCWTG as discussed above [21], although with some modifications. These modifications take into account the fact that a PV generator is interfaced through a single inverter, unlike a back-to-back inverter used for a FCWTG.

3.1.4 Central solar thermal generator (CST)

A CST is basically a conventional synchronous generator being fed by the steam produced by the heat from sun. Therefore, CST is modeled just like a fossil-fuel fired plant with separate models for generator, exciter and turbine.

3.2 Modeling and Control of Wind Generators

The following section gives the modeling details of various types of wind generators as used in the GE-PSLF program [22].

3.2.1 Doubly fed induction generator dynamic models

The power flow provides the initial conditions for dynamic simulations. The dynamic models take into account generator, power electronics converter and turbine models.

Generator/ Converter model

This model is the equivalent of the generator and field converter, differing from conventional generator models in the sense that it does not have any mechanical state variables for the rotor, which are instead included in the turbine model. Such a model is shown in Figure 3.4 [22].

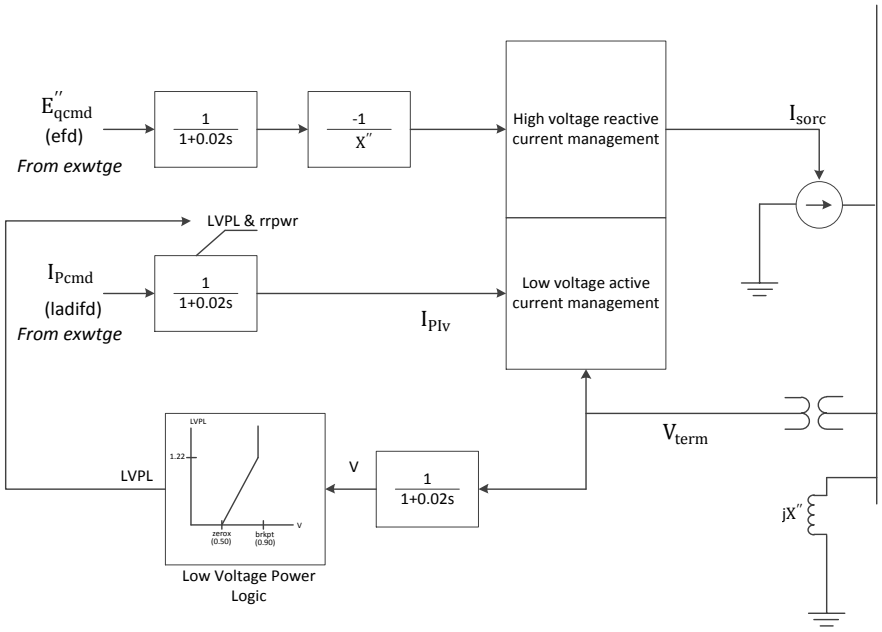

Figure 3.4 DFIG generator/converter model [22]

This model is effectively a controlled-current source that calculates the required injected current into the network by responding to the flux and active current commands from the electrical control model. There also is a low voltage power logic and fast-acting converter controls that eliminate over-voltage condi-

tions by reducing reactive current output. The model holds constant both the active power current component and the voltage behind the effective generator sub-transient reactance. The high voltage reactive current management function limits excess voltage on generator terminals by suppressing reactive current injection during over-voltage conditions.

Converter control model

This model controls the active and reactive power to be delivered to the network. Such a model is shown in Figure 3.5 [22].

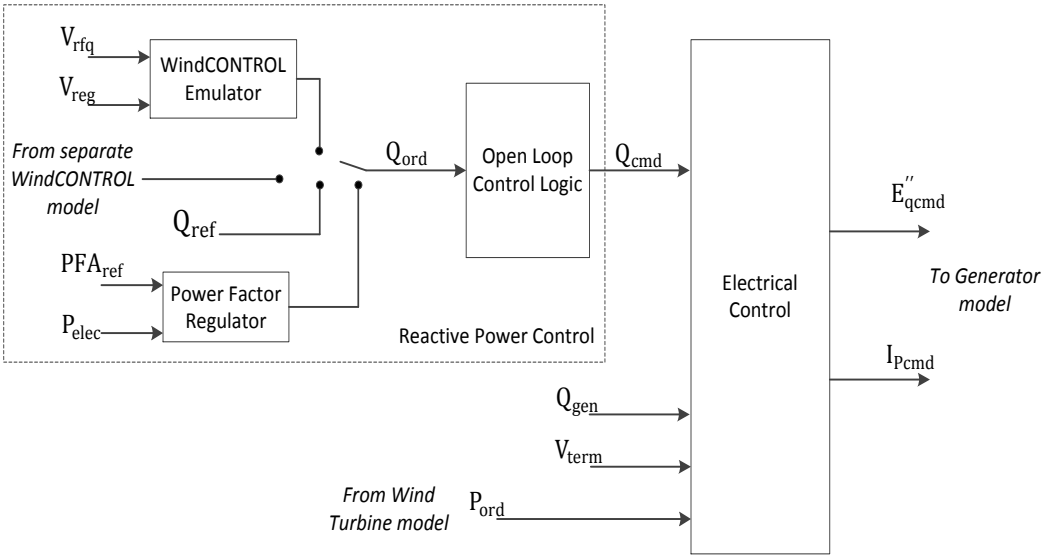

Figure 3.5 Full converter generator/converter model [22]

Reactive power control is accomplished by following one of the two control philosophies [22],

- Comparing the voltage at the specified bus against the reference voltage and regulating the voltage using PI controller, with appropriate time constants to account for the control delays
- Keeping power factor constant by using a power factor regulator

The output signal of the reactive power control block, Q_{cmd}, is compared to the reactive power generated by the converter and the error signal thus obtained is integrated with an integral gain to generate a reference voltage, V_{ref}. This voltage reference is compared to the terminal voltage and the resulting voltage error is integrated with another integral gain to generate voltage command, E''_{qcmd}, which is then fed to the generator model. An additional input signal to the generator model, I_{Pcmd}, is computed from the wind turbine model power order and terminal voltage.

Wind turbine and turbine control model

The wind turbine model represents the controls and mechanical dynamics of the wind turbine such that maximum power is extracted from the available wind without exceeding equipment rating. This model governs the mechanical shaft power, which itself is dependent on wind velocity, rotor speed and blade pitch.

The turbine control model sends a power order to the electrical control to deliver assigned power to the network. The turbine speed control is approximated by a closed loop control with a speed reference that is proportional to electric

power output. The normal value of reference speed is 1.2 p.u. at rated wind speed, but for power output levels below 46%, the reference speed is evaluated as follows [22],

$$\omega_{\text{ref}} = -0.75\text{P}^2 + 1.59\text{P} + 0.63 \tag{3.4}$$

The rotor model computes the rotor speed by using mechanical power from the wind power model and electrical power from generator/converter model. The wind power model calculates the shaft mechanical power from the wind energy, using the following equation [22],

$$P = \frac{\rho}{2} A_r v_\omega^3 C_p(\mu, \theta) \tag{3.5}$$

where, P is the mechanical power extracted from the wind, ρ is the air density in kg/m^3, A_r is the area swept by the rotor blades in m^2, v_ω is the wind speed in m/sec, C_p is the power coefficient, μ is the ratio of the rotor blade tip speed and the wind speed, and θ is the blade pitch angle in degrees.

3.2.2 Full converter generator dynamic models [22]

Generator/ Converter model

This model for full converter wind turbines is similar to that of the DFIG, except that the full converter model is represented by both active and reactive current commands. Such a model is shown in Figure 3.6.

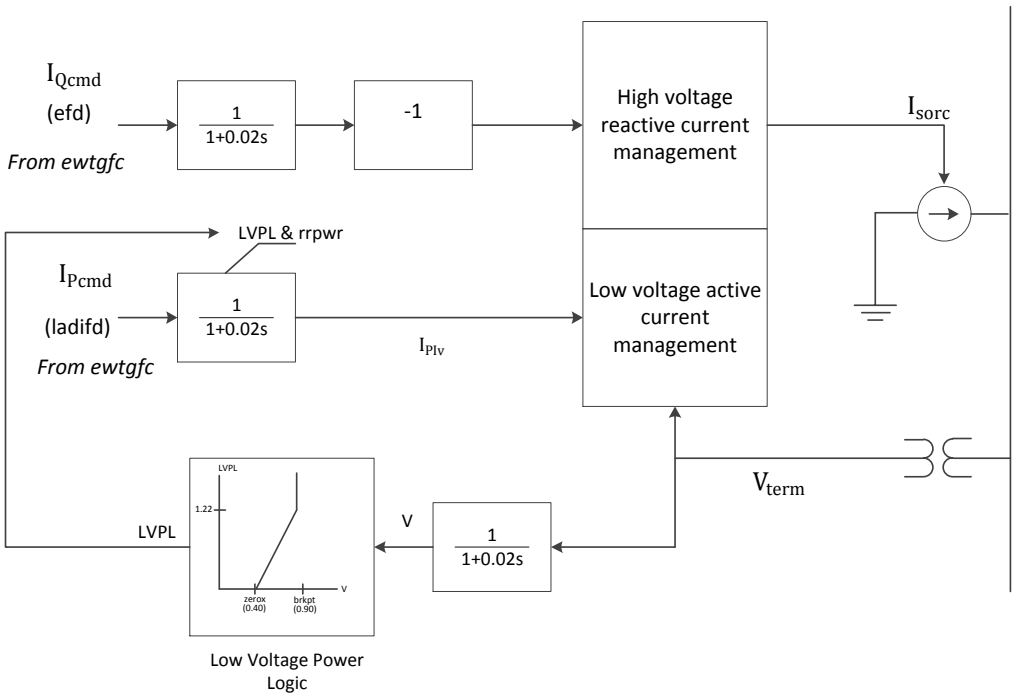

Figure 3.6 Full converter generator/converter model

Converter control model

The only difference in this model from the DFIG model is in the electrical control block, with the reactive power control unchanged. The changes for this model are to generate a reactive current command rather than a flux command and the addition of dynamic braking resistor and converter current limit.

The dynamic braking resistor minimizes the full converter WTG response to large system disturbances, such as prolonged low voltage periods, by absorbing energy in the braking resistor when the power order from wind turbine model is much greater than the electrical power delivered to the grid. Converter current limit function prevents the active and reactive current combination from exceeding converter capability.

Wind turbine and turbine control model

The same model is used for full converter WTG as that for DFIG, along with the addition of dynamic braking resistor and implementation of no-wind (zero power) VAr capability. The signal representing the dynamic braking resistor power is added to the electrical power as an input to both the rotor model and the creation of speed reference [22].

3.3 Power system stability

Power system stability may be broadly defined as that property of a power system that enables it to remain in a state of operating equilibrium under normal operating conditions and to regain an acceptable state of equilibrium after being subjected to a disturbance [23]. Under steady state conditions, there is equilibrium between the input mechanical torque and the output electrical torque of each machine, and the speed remains constant. If the system is perturbed, this equilibrium is upset, resulting in acceleration or deceleration of the rotors of the machines.

In an interconnected power system, the rotor angle stability of each synchronous machine dictates the ability to restore equilibrium. Wind and solar PV plants, being inherently asynchronous in nature, change the system dynamics with respect to the interaction of synchronous machine rotors among themselves. The mechanism associated with generation of electricity from wind and solar resources, together with their interface with the bulk power contributes to change in system dynamics.

The mechanism by which interconnected synchronous machines maintain synchronism with one another is through restoring forces, which act whenever there are forces tending to accelerate or decelerate one or more machines with respect to other machines. The change in electrical torque of a synchronous machine following a perturbation can be resolved into two components [23]:

- Synchronizing torque component, which is in phase with the rotor angle perturbation
- Damping torque component, which is in phase with the rotor speed deviation

System stability depends on the existence of both components of torque for each of the synchronous machines. Lack of sufficient synchronizing torque results in instability through an aperiodic drift in rotor angle, while lack of sufficient damping torque results in oscillatory torque. For convenience in analysis and for gaining useful insight into the nature of stability problems, the rotor angle stability is further categorized into transient stability and small signal stability.

3.3.1 Transient stability

Transient stability is the ability of a power system to maintain synchronism when subjected to a severe disturbance such as a fault on transmission facilities, loss of generation, or loss of a large load. The system response to such disturbances involves large excursions of generator rotor angles, power flows, bus voltages and other system variables. The resulting system response is influenced by the nonlinear characteristics of the power system. If the resulting angular sepa-

ration between the machines in the system remains within certain bounds, the system maintains synchronism. Transient stability depends on both the initial operating state of the system and the severity of the disturbance. Instability is usually caused due to insufficient synchronizing torque and results in aperiodic angular separation. The time frame of interest in transient stability studies is usually 3 to 5 seconds of the initial disturbance [23].

In a synchronous machine, if due to a disturbance the rotor speed increases, it causes a corresponding increase in rotor angle also. This increase in rotor angle results in an increase in electrical load on the generator. This load increase provides a synchronizing torque to the rotor and helps to bring the rotor back to synchronism. In the case of asynchronously connected wind generators, such synchronizing torque is not available to the rotor after a disturbance [25]. Therefore, the transient stability of a system with appreciable wind resources is markedly different from a system with negligible wind resources.

3.3.2 Small signal stability

Small signal stability is the ability of the power system to maintain synchronism under small disturbances, which occur continually on the system because of small variations in loads and generations. The disturbances are considered sufficiently small for linearization of system equations to be permissible for purposes of analysis. Instability that may result can be of two forms: (i) steady increase in rotor angle due to lack of sufficient synchronizing torque, or (ii) rotor

oscillations of increasing amplitude due to lack of sufficient damping torque. The nature of system response to small disturbances depends on a number of factors including the initial operating conditions, the transmission system strength, and the type of generator excitation controls used [23].

The behavior of a dynamic power system can be described by a set of n first order nonlinear ordinary differential equations of the following form:

$$\dot{x}_l = f_l(x_1, x_2, \dots, x_n; u_1, u_2, \dots, u_r; t) \quad l = 1,2, \dots, n \tag{3.6}$$

where, *n* is the order of the system and *r* is the number of inputs. This can be written in the following form by using vector-matrix notation:

$$\dot{x} = f(x, u, t) \tag{3.7}$$

where,

$$x = \begin{bmatrix} x_1 \\ x_2 \\ . \\ x_n \end{bmatrix} \qquad u = \begin{bmatrix} u_1 \\ u_2 \\ . \\ u_r \end{bmatrix} \qquad f = \begin{bmatrix} f_1 \\ f_2 \\ . \\ f_n \end{bmatrix}$$

The column vector *x* is referred to as the state vector, and its entries as state variables. The column vector *u* is the vector of inputs to the system.

The output variables can be expressed in terms of the state variables and the input variables in the following form:

$$y = g(x, u) \tag{3.8}$$

where,

$$y = \begin{bmatrix} y_1 \\ y_2 \\ . \\ y_m \end{bmatrix} \qquad x = \begin{bmatrix} g_1 \\ g_2 \\ . \\ g_m \end{bmatrix}$$

The column vector *y* is the vector of outputs, and *g* is a vector of nonlinear functions relating state and input variables to output variables.

The above nonlinear equations are linearized around a specific operating point for small signal stability analysis. Suppose x_0 be the initial state vector and u_0 the input vector corresponding to the equilibrium point about which the small-signal performance is to be investigated. Therefore,

$$\dot{x} = f(x_0, u_0) \tag{3.9}$$

If the system is perturbed from the operating state, by letting

$$x = x_0 + \Delta x \qquad u = u_0 + \Delta u \tag{3.10}$$

The new state can be expressed as

$$\dot{x} = \dot{x_0} + \Delta\dot{x} = f[(x_0 + \Delta x), (u_0 + \Delta u)] \tag{3.11}$$

As the perturbations are small, the nonlinear functions can be expressed in terms of Taylor's series expansion, which gives the linearized equation in the following form:

$$\Delta\dot{x_l} = \frac{\partial f_l}{\partial x_1}\Delta x_1 + \cdots + \frac{\partial f_l}{\partial x_n}\Delta x_n + \frac{\partial f_l}{\partial u_1}\Delta u_1 + \cdots + \frac{\partial f_l}{\partial u_r}\Delta u_r \tag{3.12}$$

$$\Delta y_j = \frac{\partial g_j}{\partial x_1}\Delta x_1 + \cdots + \frac{\partial g_j}{\partial x_n}\Delta x_n + \frac{\partial g_j}{\partial u_1}\Delta u_1 + \cdots + \frac{\partial g_j}{\partial u_r}\Delta u_r \tag{3.13}$$

where, n is the order of the system and r is the number of inputs. The linearized equation can be written in the form,

$$\Delta\dot{x} = A\Delta x + B\Delta u \tag{3.14}$$

$$\Delta y = C\Delta x + D\Delta u \tag{3.15}$$

where, A, B, C and D are known as state or plant matrix, control or input matrix, output matrix and feed forward matrix respectively.

By taking the Laplace transform of the above equations, the state equations in frequency domain are obtained:

$$s\Delta x(s) - \Delta x(0) = A\Delta x(s) + B\Delta u(s) \tag{3.16}$$

$$\Delta y(s) = C\Delta x(s) + D\Delta u(s) \tag{3.17}$$

$$(sI - A)\Delta x(s) = \Delta x(0) + B\Delta u(s) \tag{3.18}$$

The poles of $\Delta x(s)$ and $\Delta y(s)$ are the roots of the equation

$$\det(sI - A) = 0 \tag{3.19}$$

The values of *s* which satisfy the above equation are known as eigenvalues of matrix *A*, and the above equation is referred to as the characteristic equation of matrix *A*.

The time dependent characteristic of a mode corresponding to an eigenvalue λ is given by $e^{\lambda t}$. A real eigenvalue corresponds to a non-oscillatory mode and a negative real eigenvalue represents a decaying mode, while a positive real eigenvalue represents aperiodic instability. Complex eigenvalues occur in conjugate pairs and each pair corresponds to an oscillatory mode. The real part of the

eigenvalue gives the damping, and the imaginary part gives the frequency of oscillation. A negative real part represents a damped oscillation, while a positive real part represents oscillation of increasing amplitude. For a complex pair of eigenvalues:

$$\lambda = \alpha \pm j\beta \tag{3.20}$$

The frequency of oscillation (f) and damping ratio (ξ) are given by,

$$f = \frac{\omega}{2\pi} \tag{3.21}$$

$$\xi = \frac{-\alpha}{\sqrt{\alpha^2 + \beta^2}}. \tag{3.22}$$

An eigenvalue of the state matrix *A* and the associated right eigenvector (ϕ_i) and left eigenvector (ψ_i) are defined as,

$$A\phi_i = \lambda_i \phi_i \tag{3.23}$$

$$\psi_i A = \lambda_i \psi_i \tag{3.24}$$

The right eigenvector gives the mode shape, that is, the relative activity of the state variables when a particular mode is excited. For example, the degree of activity of the state variable x_k in the i^{th} mode is given by the element ϕ_{ki} of right eigenvector ϕ_i. The k^{th} element of the left eigenvector ψ_i weighs the contribution of this activity to the i^{th} mode. The participation factor of the k^{th} state variable x_k in the i^{th} mode is defined as the product of the k^{th}component of the right and left eigenvectors corresponding to the i^{th} mode,

$$p_{ki} = \phi_{ki}\psi_{ik} \tag{3.25}$$

In large power systems, the small-signal stability problem can be either local or global in nature. Local plant mode oscillations are associated with rotor angle oscillations of a single generator or a single plant against the rest of the system. Local problems may also be associated with oscillations between the rotors of a few generators close to each other. These oscillations have frequencies in the range of 0.7 to 2.0 Hz [23]. On the other hand, global small-signal stability problems are caused by interactions among large groups of generators and have widespread effects. They involve oscillations of a group of generators in one area swinging against a group of generators in another area. Such inter-area oscillations have frequencies in the range of 0.1 to 0.7 Hz [23].

As wind and solar PV generation resources inject power asynchronously to the grid, they affect the electromechanical modes of oscillations of other synchronous machines in the system, even though they themselves do not participate in such modes.

Chapter 4. PROPOSED APPROACH FOR RESEARCH

An increase in renewable generation resources within the study area is accompanied by a corresponding decrease in generation from conventional fossil fuel fired power plants through retirement. Therefore, the number of conventional generators decreases along with a decrease in total system inertia. The present work deals with transient stability assessment of these remaining conventional generators as affected by interaction with the renewable energy resources. To accomplish this, three phase faults are applied at suitably chosen locations throughout the study area and the rotor angular response of the remaining synchronous machines is observed. If the rotor oscillations settle down to new angular positions and are properly damped, then the system can be considered to be transiently stable for that particular fault condition. Small signal stability studies are also done to observe the inter-area modes affected due to renewable integration. The power flow and transient stability studies are conducted using PSLF program V17.0, a tool developed by GE [26]. The small signal study is done using SSAT which is part of DSA^{Tools}, a tool developed by Powertech Labs Inc. [27].

4.1 System description

The study is carried out on a large system having 17686 buses, 8476 loads and 3818 generators with a total installed capacity of 308,556 MW. Within this large system, the study area where new renewable resources are being installed has a total installed capacity of 47,090 MW. Two operating cases of the system

are studied depending upon whether wind generation is at its maximum or solar generation is at its maximum. These cases are referred from now onwards as:

i. "Max Solar case"

ii. "Max Wind case"

The Max Solar case is built-off the peak load case but represents a scenario in which the solar penetration in the study area is represented to its maximum capacity. The Max Wind case is built-off the off-peak load case but represents a scenario in which the wind penetration in the study area is represented to its maximum capacity. Max Wind case corresponds to the system load in early morning hours, hence accounting for the generation from solar resources. Table 4.1 summarizes the two cases.

Table 4.1 Max Solar and Max Wind case description

Cases	**Study area load, MW**	**Study area generation, MW**	**Study area PV generation, MW**	**Study area CST generation, MW**	**Study area wind generation, MW**
Max Solar	26,478	21,450	1,134	3,737	2,446
Max Wind	12,908	11,259	1,593	1,758	3,768

For the two study cases, the wind resources are modeled using Type-3 and Type-4 models for GE 1.5 MW models available within PSLF. The solar thermal resources are modeled using conventional round rotor models for synchronous

machines along with their exciters and turbine governors. Solar PV resources are modeled using an EPCL program within PSLF to model network current injection for the solar PV inverter.

4.2 Contingency analysis

A detailed contingency analysis of both the cases is conducted using SSTOOLS feature within PSLF. Static *N-1* and *N-2* contingency studies are conducted to identify contingencies which cause post-disturbance steady state violations with regard to voltage limits, flow limits, and non-convergence. The studies serve to provide the most stressed points within the network, which may be sensitive to system disturbances. These results are then used as a guide to select cases for transient stability analysis.

4.3 Transient stability studies

The most severe contingencies as obtained from contingency screening are then studied from the point of view of transient stability. In addition to the critical cases identified by the static contingency analysis study, all the major transmission lines within the study area are also considered. These studies consist of applying three phase faults at a bus at one end of the identified transmission corridor and clearing the fault by opening the line. The clearing times used to conduct the study are:

500 kV and 345 kV – 4-cycle clearing

230 kV – 6-cycle clearing

115 kV – 6-cycle clearing

4.4 Reduced reserve margin studies

Given the large penetration of wind and solar resources, analysis is also conducted to examine the impact of reserve requirement on system performance and on the ability to reach a post-disturbance steady state following the loss of significant amounts of wind or solar generation. The reserve generation available within the original system is about 29%. This is significantly higher than the reserve generally used in operational practice. For the Max Wind and the Max Solar cases, the reserve in the study area is reduced to 10% based on the following relationship:

$$\frac{\sum P_{max} - \sum P_{gen} - \sum P_{import}}{\sum P_{gen}} = 0.1 \tag{4.1}$$

where, P_{max} is the maximum output rating of each unit, P_{gen} is the plant output specified in the power flow case considered, and P_{import} is the real power being imported in the study area. The units with the maximum difference between P_{max} and P_{gen} are shut down. In addition some negative generation units are also shut down to maintain balance between generation and load. The imports into the study area are held constant. Based on this approach the conditions after implementing the reduction in reserve to 10% for the Max Wind and the Max Solar cases are shown in Table 4.2.

Table 4.2 Operating conditions with reduced reserves

	Max Wind Case		Max Solar Case	
	Original case	Reduced reserve case	Original case	Reduced reserve case
∑ Pmax (MW)	17,501.1	14,462.6	27,822.5	25,452.5
∑ Pgen (MW)	11,260	11,230.4	21,449.9	21,418.7
Net imports (MW)	2007	2007	5656.2	5656.7

Additionally, to examine the combined effect of reduced system reserve and reduced system inertia, all the CST plants are replaced with PV solar plants.

4.5 Explanation of results

The results obtained in the previous sections are scrutinized to provide reasoning behind the research findings and results. The purpose of these studies is to investigate the dynamic behavior of the system for a disturbance from the point of view of initial steady state rotor angles of the synchronous machines in the system. The extent to which renewable generation resources impact the system can be assessed by comparing the Max Solar and Max Wind cases with the corresponding cases having no renewables at all. Therefore, two new cases with no renewable generation resources are prepared corresponding to system peak load and off-peak load conditions. The rest of the generators in these new cases are dispatched to ensure balance with the corresponding load levels. The peak load case is compared to the Max Solar case and the off-peak load case is compared to the Max Wind case.

4.6 Small signal stability studies

The purpose of these studies is to investigate the effect of renewable generation resources on most critical inter-area modes of rotor oscillations. If an inter-area mode is not well damped, the steady state power transfer capability between the two areas is limited. In addition, a poorly damped mode of oscillation may be detrimental to system stability if that mode is excited by some disturbance in the system. The most critical modes are found by performing complete eigenvalue analysis using SSAT. As explained in previous section, the impact of renewable generation resources can be assessed by comparing with the system with no renewables at all.

Chapter 5. RESULTS AND DISCUSSION

5.1 System description

The area under study, designated as Area -1, is shown in Figure 5.1 along with interfaces with surrounding areas. This diagram shows the most critical 500 kV lines within the system, along with some critical 230 kV and 115 kV buses connected to 500 kV buses through step-down transformers. Various renewable resources to be added to the system are represented as equivalent hubs. Wind-1 and Wind-2 are the hubs for wind generation resources, while Solar-1, Solar-2, Solar-3, Solar-4 and Solar-5 are the hubs for PV and CST generation resources.

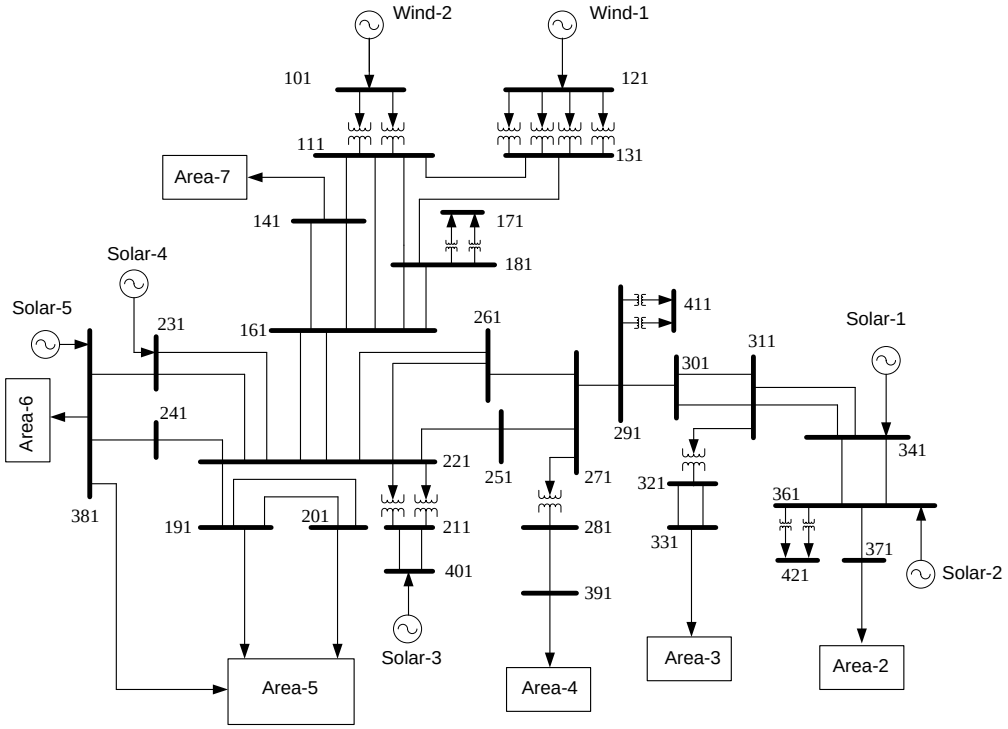

Figure 5.1 Single line diagram showing the major transmission lines and buses within study Area-1

The contingency study for transmission lines within Area-1 and at the interfaces with surrounding areas provides a list of critical contingencies to examine. The transient stability study results for these contingencies are shown in the following sections.

5.2 Transient stability results

Most of the *N-1* contingencies do not give significant transient instability results. Therefore, only *N-2* contingencies are considered. A contingency is applied by placing a bus fault at one end of a transmission line with the subsequent opening of that line along with one more line after the designated fault duration. The following section gives the plots for critical contingencies and their accompanying explanations. The results are presented for the Max Solar and Max Wind cases separately.

5.2.1 Max Solar case

Max solar case is a highly stressed case and a number of contingencies cause significant problems. Table 5.1 lists the critical contingencies identified for this case and the transient stability results for these contingencies. The table also lists the possible protection methods to be used in case such contingencies occur.

Table 5.1 Summary of transient stability analysis for the Max Solar case

Contingency #	Contingency Description	Results	Solution
1	291(bf) -271, 371 - 361	Angle instability at several units in Areas-1, 3	Dropping some CST units in Solar-2 and Solar-4 hubs stabilizes the system
2	291 (bf)- 301, 371- 361	Angle instability at several units in Areas-1, 3	Dropping some CST units in Solar-2 and Solar-4 hubs stabilizes the system
3	311 (bf) - 341 (double ckt.)	Angle instability of several CST units in Solar-1 and Solar-2 hubs	Dropping CST units in Solar-2 hub stabilizes the system
4	321 (bf) - 331 (double ckt.)	Angle instability of several units in Area-1 and 3	System does not stabilize
5	221 (bf)-211– both transformers outaged	Angle instability of several generators in Area 1	System does not stabilize

(bf): bus fault

As shown in Figure 5.2 and Figure 5.3, some of these contingencies result in significant loss of synchronism. Contingencies # 1-3 are stabilized by dropping some CST units in Solar-2 and Solar-4 hubs. However, Contingencies # 4-5 are not stabilized and should be considered as serious contingencies for the system. Another fault case depicting a severe bus fault at bus 111 near Wind-2 hub and cleared by opening the lines to 131and 181 buses does not cause any loss in rotor angle stability. This case is shown in Figure 5.4.

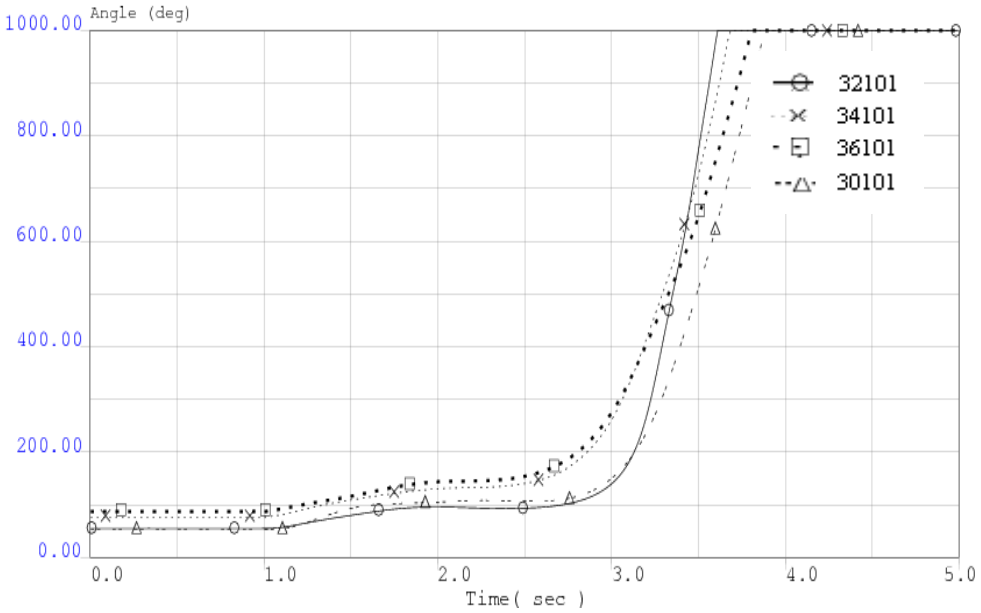

Figure 5.2 Rotor angle plots for some of the unstable generators around buses 341, 361 due to contingency#1

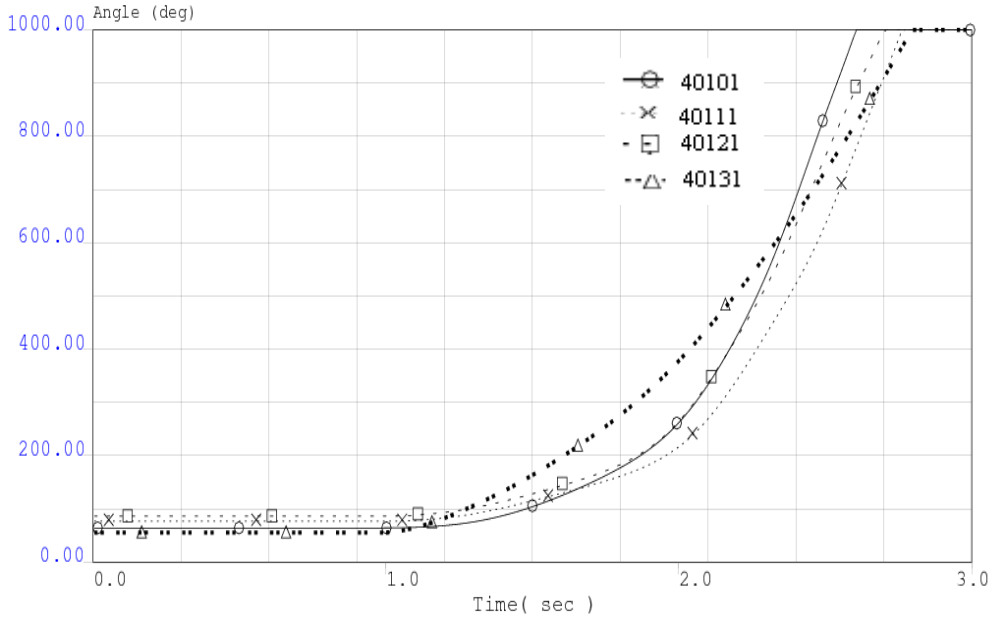

Figure 5.3 Rotor angle plots for some of the unstable generators around buses 401, 141 due to contingency#5

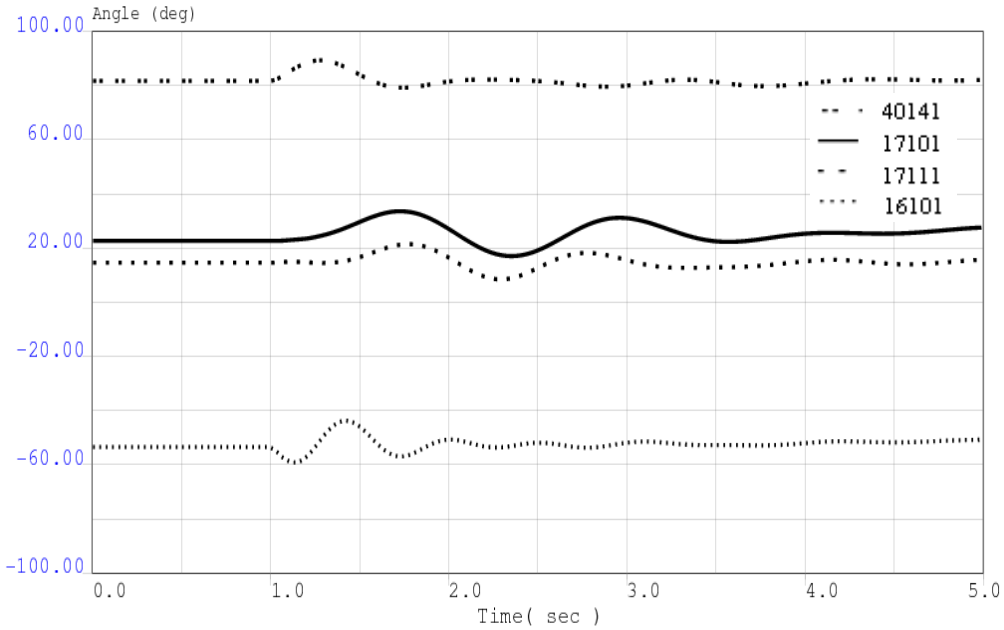

Figure 5.4 Fault case of 111(bf)-131, 181 (Stable)

5.2.2 Max Wind case

As with Max Solar case, the most critical *N-2* contingencies for Max Wind case are shown in Table 5.2.

Table 5.2 Summary of transient stability analysis for the Max Wind case

Contingency #	**Contingency Description**	**Results**
6	131(bf)- 111, 181	Angle instability at two small generators in Area-1
7	291 (bf)- 271, 301	Voltage recovery problem at bus 291
8	221 (bf)- 241, 241 -381	Voltage recovery problem at some buses
9	181 (bf)- 131, 111 - 131	Angle instability at two small generators in Area-1
10	221 (bf)-211– both transformers outaged	Angle instability at several generators in Area-1
11	311 (bf) - 341(double ckt.)	Stable
12	221 (bf) -261(double ckt.)	Stable
13	221 (bf) - 231(double ckt.)	Stable
14	361 (bf)-421–both transformers outaged	Angle instability at some CST units in Area- 1

(bf): bus fault

The Max Wind case is less severe as compared to Max Solar case, as there are only two contingencies which cause instability at several generators (Figure 5.8). Two of the contingencies (#6, 9) cause only two small generators to lose synchronism with rest of the system. One such scenario is shown in Figure 5.5. These two generators have power outputs of less than 20 MW each. Some of the contingencies cause localized voltage recovery problems, as shown in Figure 5.6. This voltage recovery problem occurs because the contingency isolates the buses 291 and 411 from rest of the grid, as shown in Figure 5.7. A stable case for a se-

vere contingency is shown in Figure 5.9 where a three phase fault taking out two critical lines near Solar-1 hub does not cause any generator to lose synchronism.

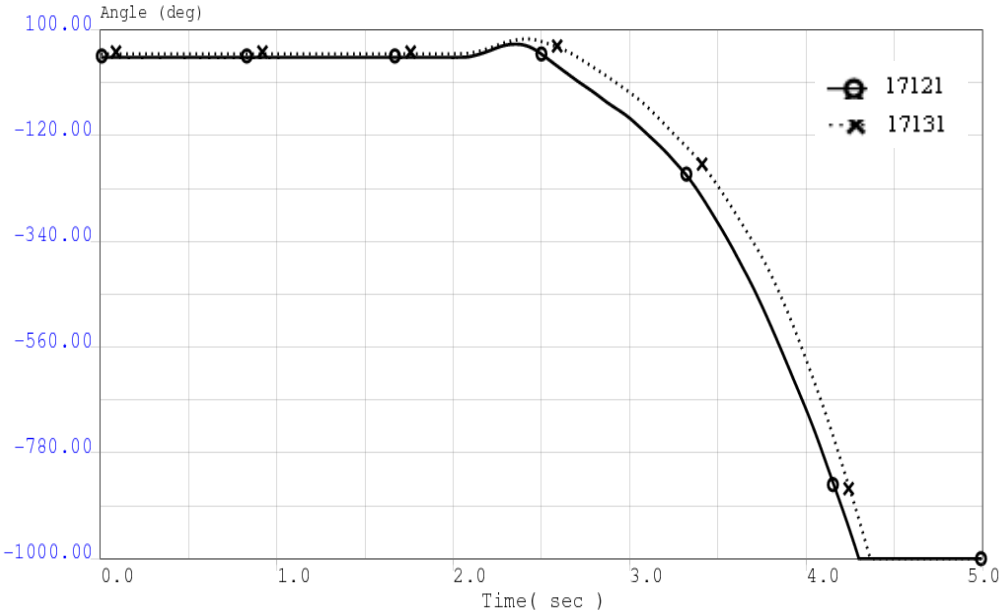

Figure 5.5 Rotor angle plots for the two unstable generators due to contingency#6

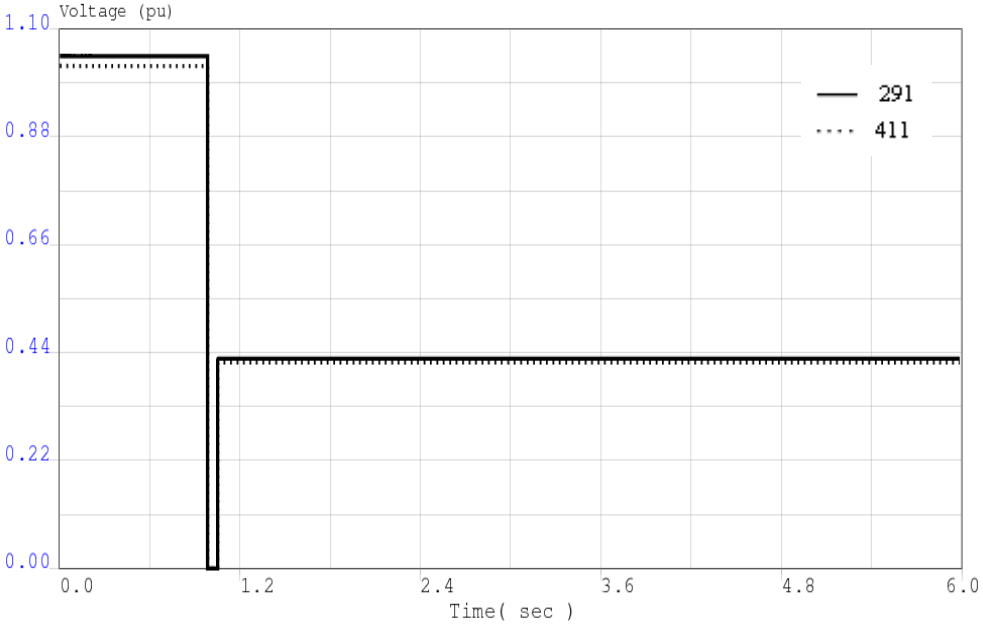

Figure 5.6 Bus voltages for buses 291, 411 due to contingency#7

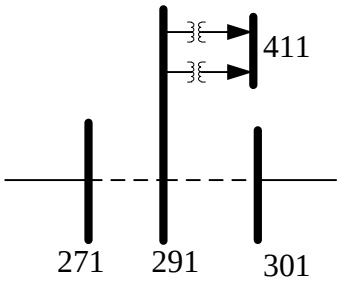

Figure 5.7 Post-disturbance network topology around bus 291 for contingency#7

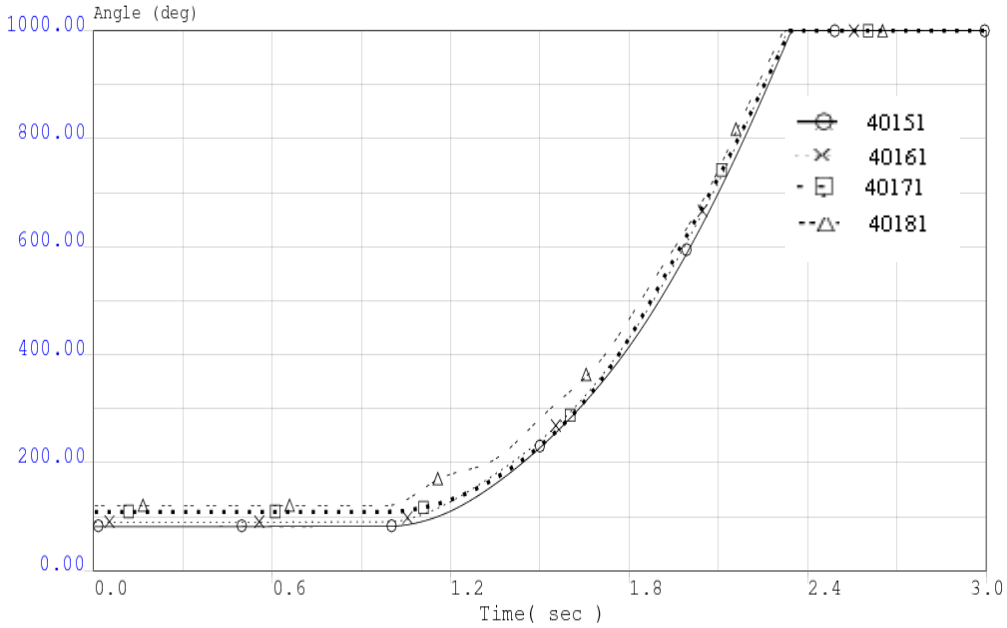

Figure 5.8 Rotor angle plots for some of the unstable generators around buses 401, 141 due to contingency#10

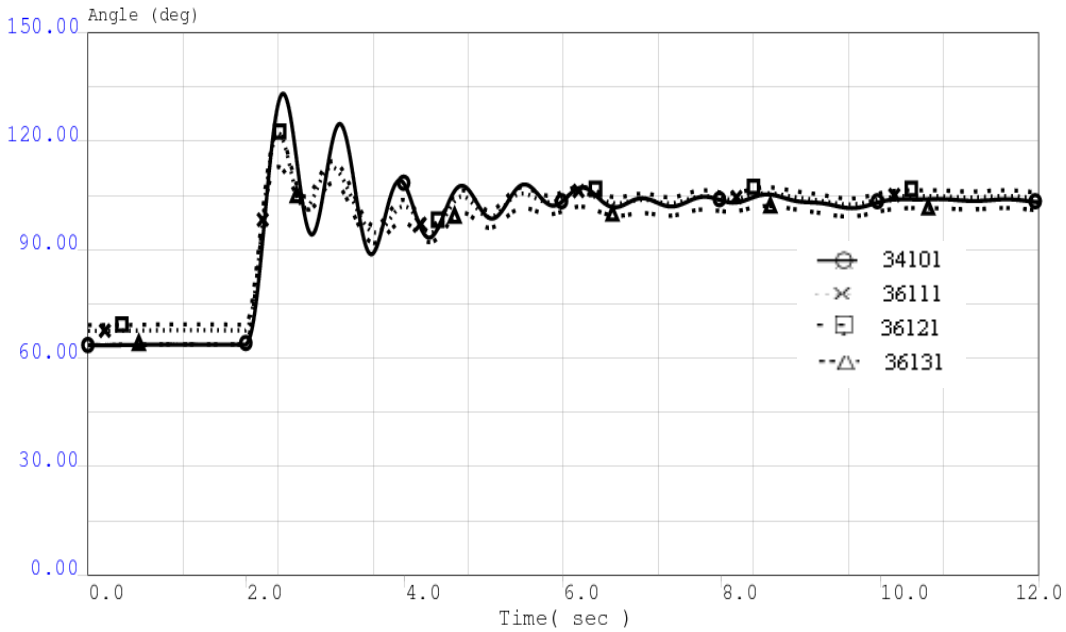

Figure 5.9 Contingency#11 depicting transient stability

5.3 Loss of renewable generation resources

Since the contingencies discussed in section 5.2 are severe disturbances, the issue of an acceptable post-disturbance equilibrium is also important. This study involves the complete loss of biggest wind and solar generation hubs respectively and the subsequent generation pick-up in neighboring areas. A post-disturbance power flow is conducted and the automatic generation adjustment feature in PSLF is invoked. The results of the power flow analysis are presented in this section.

5.3.1 Loss of Wind-1 hub generation

On removing the two 500 kV lines from bus 131 to bus 111 and bus 181, there is a complete isolation of the wind generation in the Wind-1 hub. In all, 2830 MW of generation is lost in Area-1. Subsequently in the post-disturbance

steady state solution 1000 MW is picked up by other dispatchable generators within Area-1. The remainder of the generation lost is then picked up by generators in the adjoining areas as shown in Table 5.3. The generators are re-dispatched such that none of them exceed their maximum ratings. In addition to picking up lost generation, none of the transmission lines at the interfaces exceed their ratings.

Table 5.3 Post-disturbance distribution of generation after loss of Wind-1 hub generation

Area	**Pgen in base case (MW)**	**Pgen after contingency (MW)**	**∆Pgen (MW)**
1	11213	9383	-1830
2	24172	25383	1211
6	2425	2750	325
7	10251	10514	263
4	1913	2083	170
Total	49974	50113	

5.3.2 Loss of Solar-2 hub generation

A similar study is done for the loss of Solar-2 CST hub near bus 361, involving a loss of 1494 MW of generation. Subsequently in the post-disturbance steady state solution 448 MW is picked up by other dispatchable generators within Area-1 resulting in a net loss of 1046 MW in Area-1. The remainder of the generation lost is then picked up the generators in the adjoining areas as shown in Table 5.4. Again, the re-dispatched generators and the transmission lines do not exceed their ratings.

Table 5.4 Post-disturbance distribution of generation after loss of Solar-2 hub generation

Area	**Pgen in base case (MW)**	**Pgen after contingency (MW)**	**∆Pgen (MW)**
1	21449	20403	-1046
2	30263	30788	525
6	6451	6724	273
7	3034	3120	86
4	26339	26467	128
Total	87536	87502	

5.4 Reduced reserve margin studies

5.4.1 Modified Max Solar case

The most severe contingencies for Max Solar case are compared with those of the modified case having reduced reserve and CST plants replaced by PV units with same MVA ratings. A comparison is provided in Table 5.5.

Table 5.5 Summary of reduced reserve Max Solar case with CST plants replaced by solar PV

Contingency #	**Original Max Solar case**	**Reduced reserve and CSTs replaced with solar PV case**
1	Angle instability at several units in Area-1 and 3	All machines which were unstable in original case are stable now, except two
2	Angle instability at several units in Area-1 and 3. Case diverges at 3.9 s	All machines which were unstable in original case are stable now, except two. Does not diverge
3	Angle instability of several CST units in Solar-1 and Solar-2 hubs	Network fails to converge just after fault is cleared
4	Angle instability of several units in Area-1 and 3. Diverges at 6.42 s	Same set of machines go unstable as in original case. Diverges at 2.92 s
5	Angle instability of several generators in Area-1	Same set of machines go unstable as in original case

It can be observed from Table 5.5 that certain disturbances in the reduced reserve and reduced inertia case (because of conversion of CST plants to PV solar) are more severe than the original case, and certain disturbances are more severe in the original Max Solar case. Figure 5.10 shows that the modified case is more stable than the original case, while opposite is true for Figure 5.11.

This difference in severity of disturbances depends upon how the renewable generation resources interact with the existing synchronous machines in the system. In the case of wind or PV solar, the injection source is an asynchronous source and the power electronic inverter controls the real and reactive power injection. In the case of the CST this injection is synchronous injection, controlled by the interaction of the CST synchronous generator and the remaining synchronous machines in the system. In both of the situations the remaining synchronous generators at steady state adjust their angular positions to account for the injection at the buses where renewable generation resources are connected to the grid. Therefore, the relative rotor angle difference between some generators will increase and some of them will decrease. The synchronizing capability between those generators whose rotor angle difference increases will decrease and will increase for those whose rotor angle difference reduces. In addition if the system is now subjected to a disturbance, the disturbance will affect the synchronous generators based on the location of the disturbance and its severity.

If the disturbance is close to generators whose synchronizing capability has reduced due to the two injections then these generators will be affected ad-

versely (contingency#4). On the other hand if the disturbance is located close to generators whose synchronizing capability has increased then these generators will not be affected to the same extent (contingency#1). Hence depending on the size and location of the injection due to the renewable resources, and the location and severity of the disturbance certain generators in the system will be adversely affected and some generators will be favorably affected. This phenomenon can be observed in the results shown in Table 5.5 and the accompanying plots.

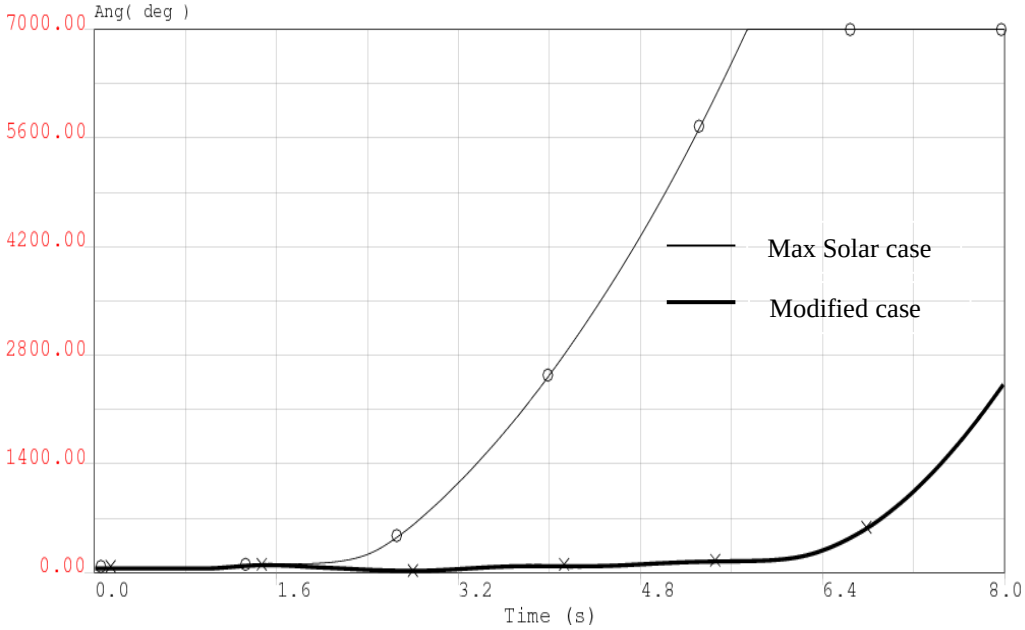

Figure 5.10 Comparison for contingency#1 showing rotor angles for a synchronous generator in Area-1 for the two cases

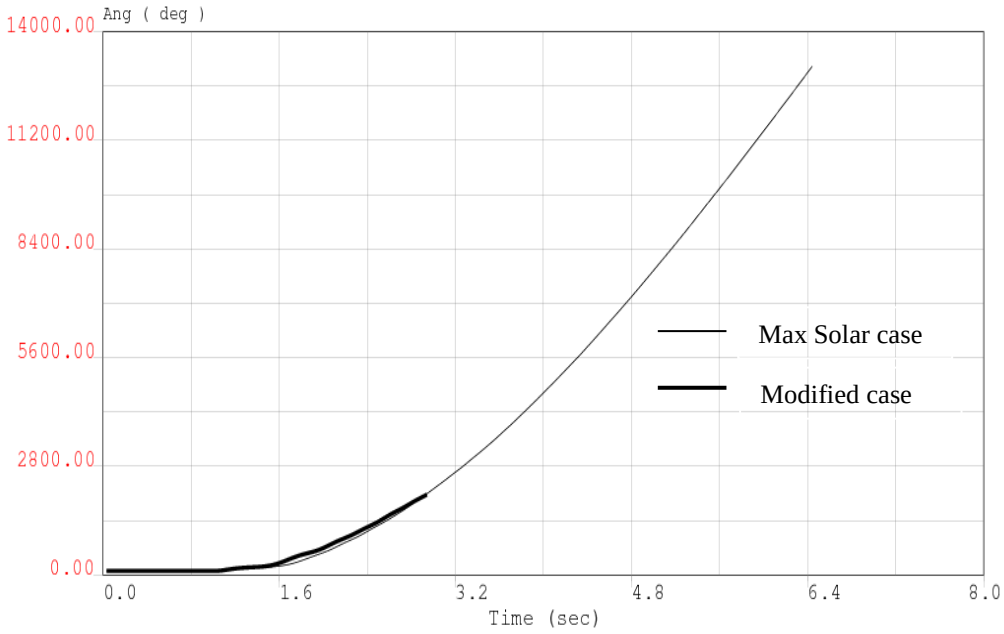

Figure 5.11 Comparison for contingency#4 showing rotor angles for a synchronous generator in Area-1 for the two cases

5.4.2 Modified Max Wind case

Similar to the Modified Max Solar case, the most severe contingencies for Max Wind case are compared with the modified case having reduced reserve and CST plants replaced by PV units with same MVA ratings. A comparison is provided in Table 5.6.

As can be observed from Table 5.6, the Modified Max Wind case shows similar general trend as the original Max Wind case in terms of dynamic performance for most of the contingencies. However, the modified case appears to be more severely affected in terms of losing synchronism earlier than the original Max Wind case, as can be seen from Figure 5.12 and Figure 5.13.

Table 5.6 Summary of reduced reserve Max Wind case with CST plants replaced by solar PV

Contingency #	**Original Max Wind case**	**Reduced reserve and CSTs replaced with solar PV case**
6	Angle instability at two small generators in Area-1	Same set of machines go unstable as in original case
9	Angle instability at two small generators in Area-1	Same set of machines go unstable as in original case
10	Angle instability of several generators in Area 1	Same set of machines go unstable as in original case
14	Some CST units go unstable in Area 1	Network fails to converge just after fault is cleared

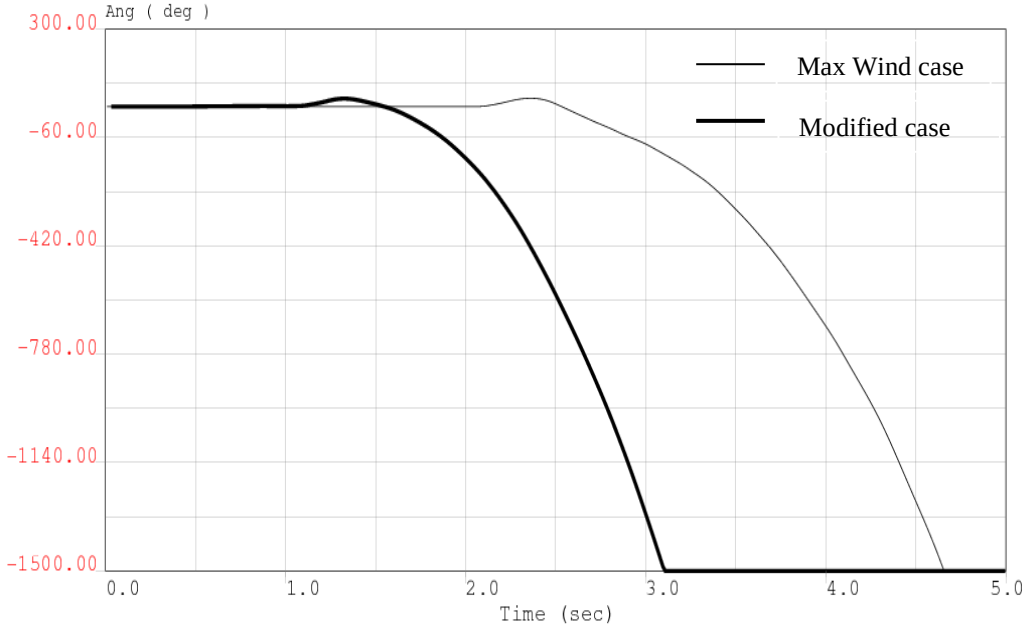

Figure 5.12 Comparison for contingency#6 showing rotor angles for a synchronous generator in Area-1 for the two cases

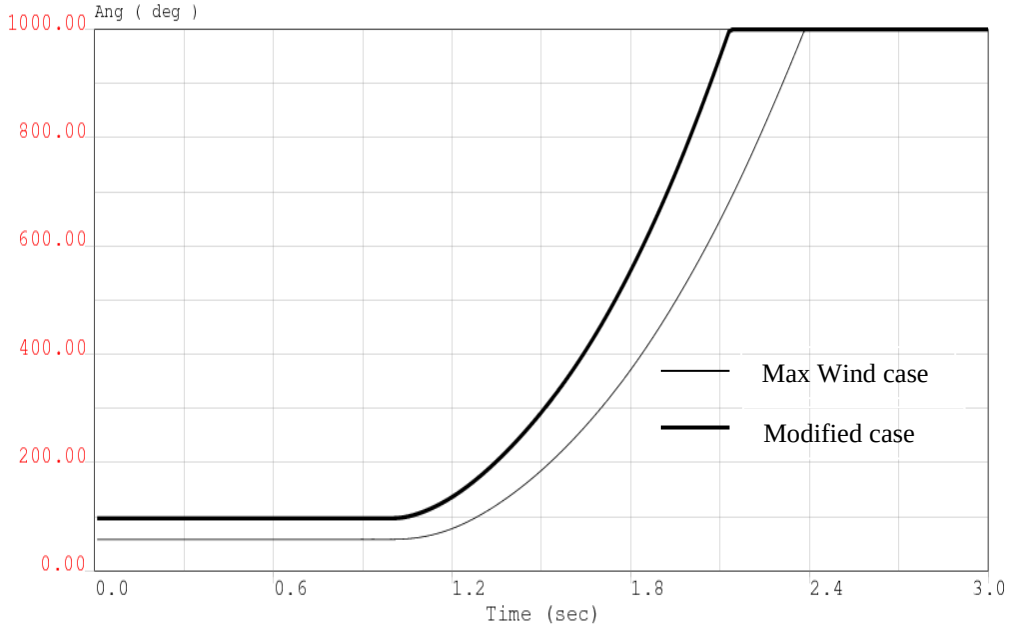

Figure 5.13 Comparison for contingency#10 showing rotor angles for a synchronous generator in Area-1 for the two cases

5.5 Explanation of results obtained in Sections 5.2-5.4

Continuing with the explanations provided in Section 5.4.1 with regards to favorable or adverse impact of renewable generation injections into the grid, further studies are conducted for the Max Solar and Max Wind cases. The peak load case with no renewables is compared to the Max Solar case and the off-peak load case with no renewables is compared to the Max Wind case.

5.5.1 Comparison of Peak case with Max Solar case

In this comparison, the first case studied is for a large synchronous generator within Area 1. This generator has a slightly higher initial relative rotor angle for the Max Solar case in comparison to the Peak case. A three phase fault is placed very close to this generator bus and cleared. The plots of the relative rotor angle of this generator for the two corresponding cases are shown in Figure 5.14. It is observed that for the Max Solar case in which this generator had a higher initial relative rotor angle, the angle swing following the same disturbance is higher in Max Solar case than for the Peak case where the initial relative rotor angle was lower. This indicates that this generator was adversely affected by the injection of the asynchronous resources and the disturbance.

To demonstrate the favorable impact of the asynchronous injection, another generator was studied. This generator has a lower initial relative rotor angle for the Max Solar case in comparison to the Peak case. A three phase fault near the generator bus causes lower relative rotor angle swings in the Max Solar case in

comparison to the Peak case. The plots for this case are shown in Figure 5.15 showing favorable impact of the asynchronous injection.

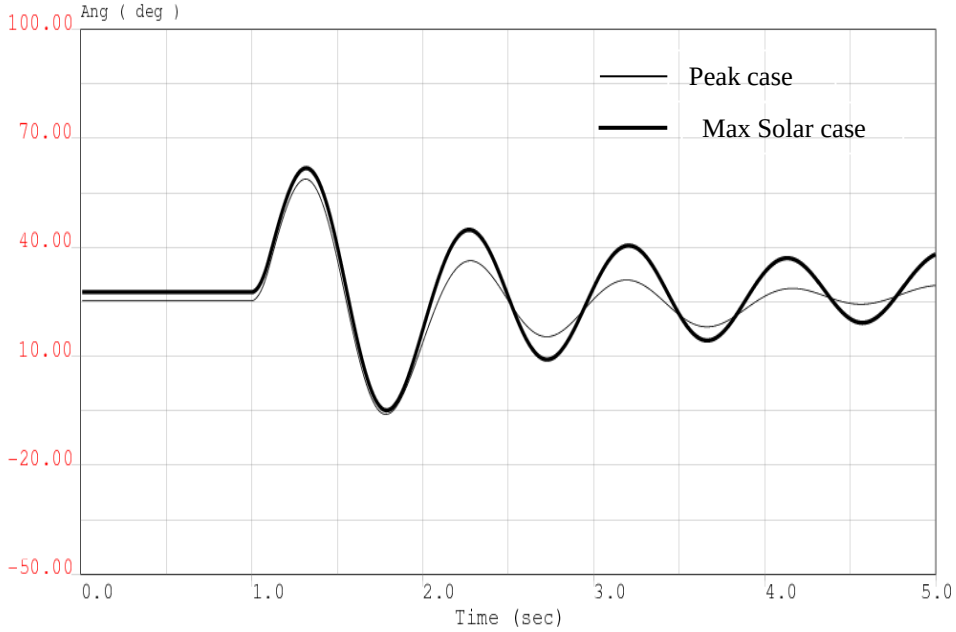

Figure 5.14 Comparison of rotor angle plots for a fault near synchronous generator 39101 for Max Solar case and Peak case showing adverse impact of renewable injection

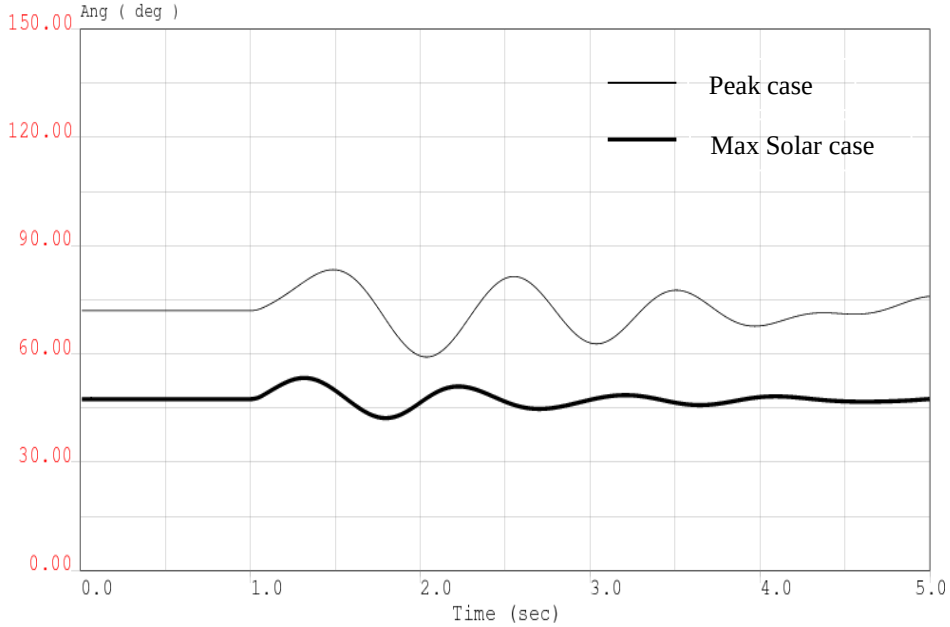

Figure 5.15 Comparison of rotor angle plots for a fault near synchronous generator 19101 for Max Solar case and Peak case showing favorable impact of renewable injection

5.5.2 Comparison of Off-peak case with Max Wind case

In this comparison, the first case considered is for a generator which has an initial relative rotor angle of 65^0 in the Off-peak case and an initial angle of 109^0 in the Max Wind case. On applying a three phase fault near the generator bus, the rotor angle plot shows higher swings for the Max Wind case in comparison to the Off-peak case, as indicated in Figure 5.16. This plot establishes the fact that the asynchronous injection from the renewable resources and the particular disturbance adversely affect this particular generator.

The favorable impact of asynchronous injection is shown by studying another generator having an initial relative rotor angle of -0.141^0 in the Off-peak case and an initial relative rotor angle of -31.715^0 in the Max Wind case. On applying the disturbance, this generator is favorably impacted by the asynchronous injection of the renewable resources as shown in Figure 5.17.

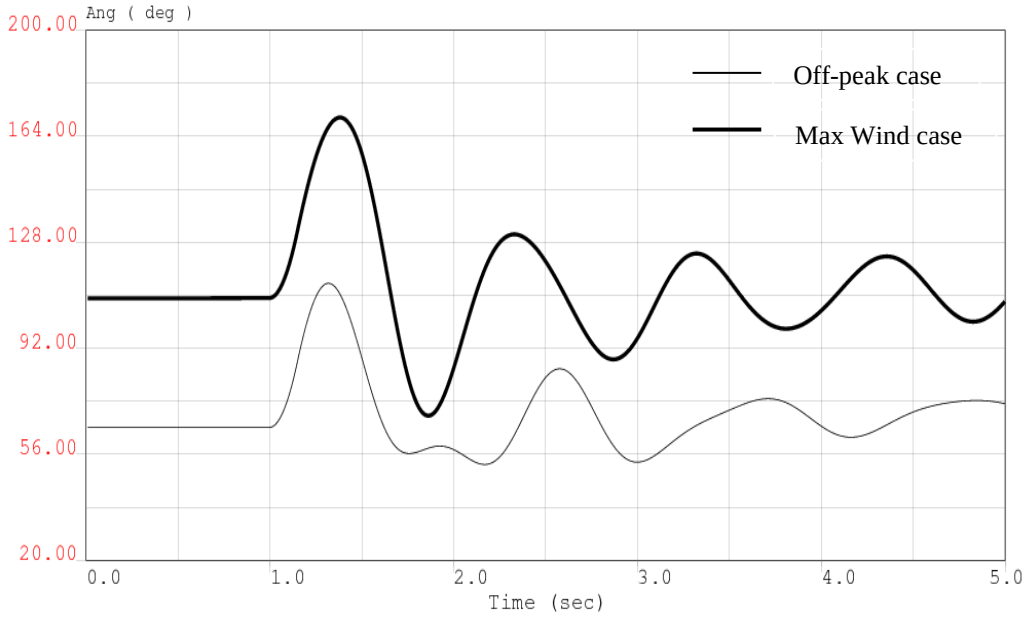

Figure 5.16 Comparison of rotor angle plots for a fault near synchronous generator 40191 for Max Wind case and Off-peak case showing adverse impact of renewable injection

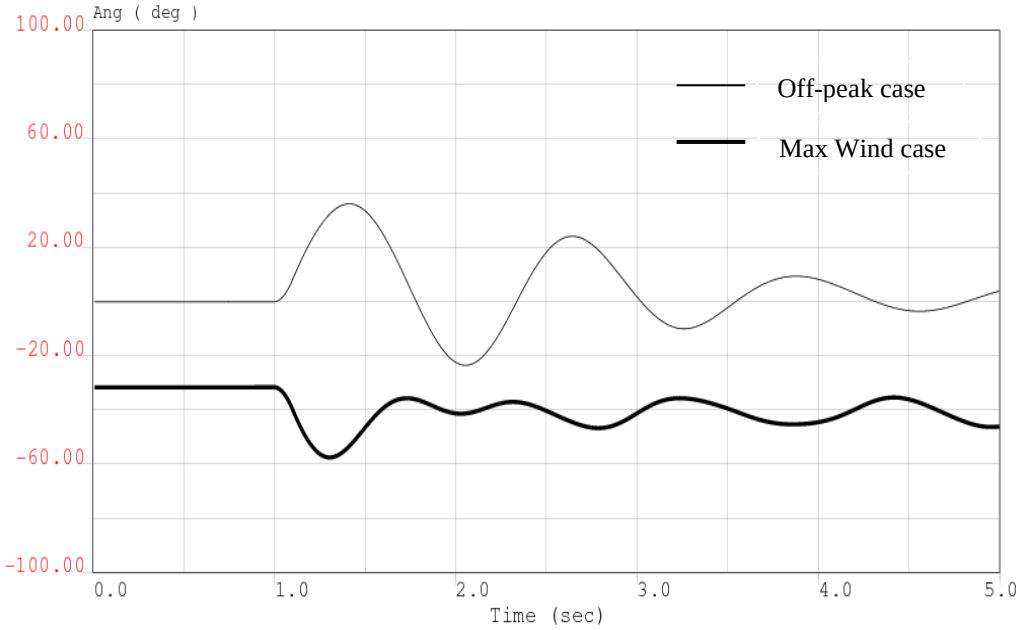

Figure 5.17 Comparison of rotor angle plots for a fault near synchronous generator 17141 for Max Wind case and Off-peak case showing favorable impact of renewable injection

5.6 Small signal stability studies

A summary of the critical inter-area modes for the entire inter-connected system is shown in Table 5.7. As can be observed from the table, the damping ratio for a corresponding mode of frequency is less for the Max Solar case than that of the Peak case, which has no renewables. Similarly, a Max Wind case mode exhibits less damping than a similar mode of the Off-peak case. Therefore, renewable penetration does affect the damping of inter-area modes.

Table 5.7 Critical mode frequencies and damping ratios

Cases	Critical mode frequency (Hz)	Critical mode damping (%)
Peak case	0.3362	10.16
	0.4751	16.12
	0.7179	5.03
Max Solar case	0.3503	1.72
	0.4814	4.58
	0.6971	2.62
Off-peak case	0.3594	12.29
	0.4681	14.12
	0.6617	4.81
Max Wind case	0.3177	1.17
	0.4755	2.31
	0.7000	2.61

To investigate the effect of these modes on the performance of study Area-1, the mode shapes and participation factors corresponding to the above modes are observed. From the participation factor plots as shown in Figure 5.18 and Figure 5.19 for Max Solar case, it is observed that mostly generators in Area-7 participate in these inter-area modes and there are no participating generators from study Area-1. A similar behavior is observed for the Max Wind plots in Figure 5.20 and

Figure 5.21. This is due to the fact that most of the renewables are added near the interface with Area-7. Hence, the effect on the inter-area modes of oscillations due to renewables is more pronounced on the Area-7 generators.

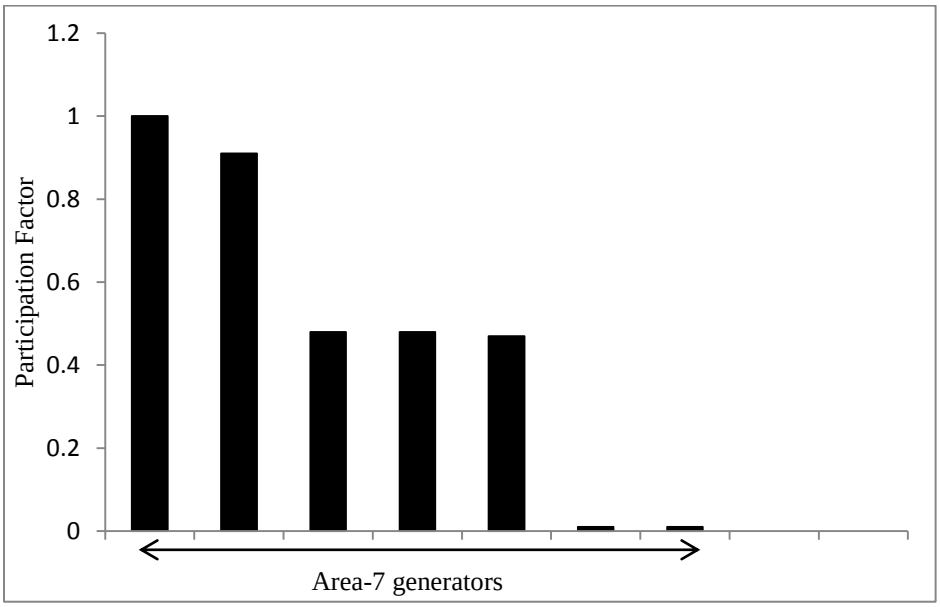

Figure 5.18 Participation factor corresponding to generator speed state for 0.3503 Hz inter-area mode in Max Solar case

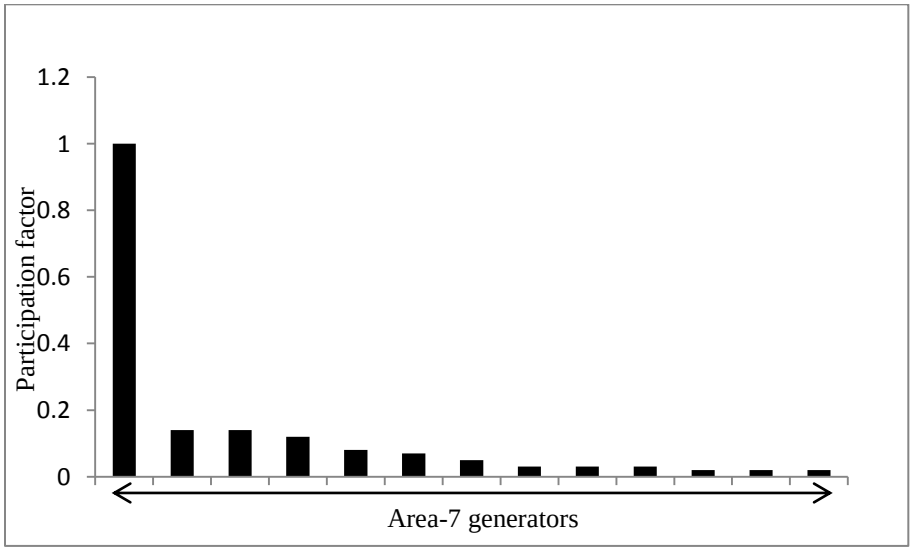

Figure 5.19 Participation factor corresponding to generator speed state for 0.4814 Hz inter-area mode in Max Solar case

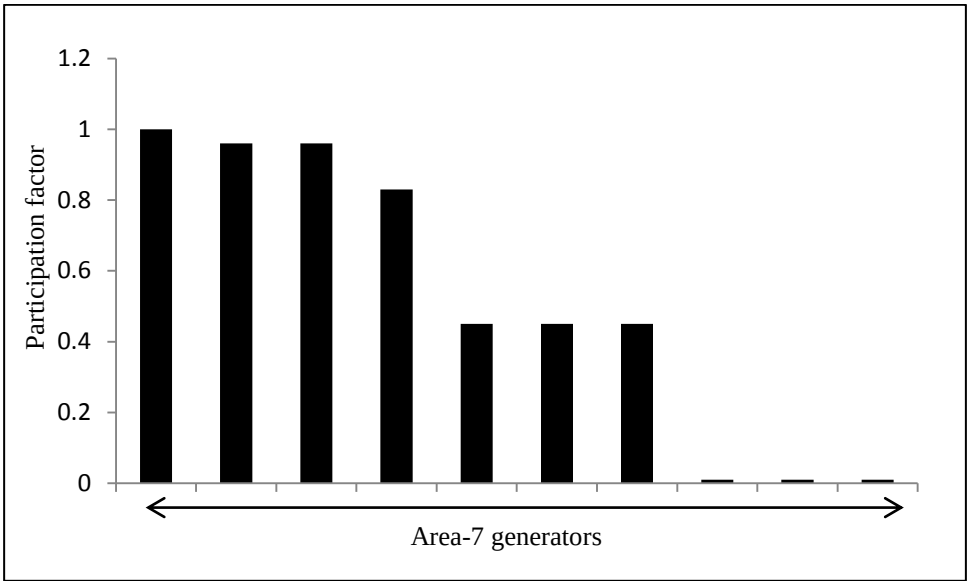

Figure 5.20 Participation factor corresponding to generator speed state for 0.3177 Hz inter-area mode in Max Wind case

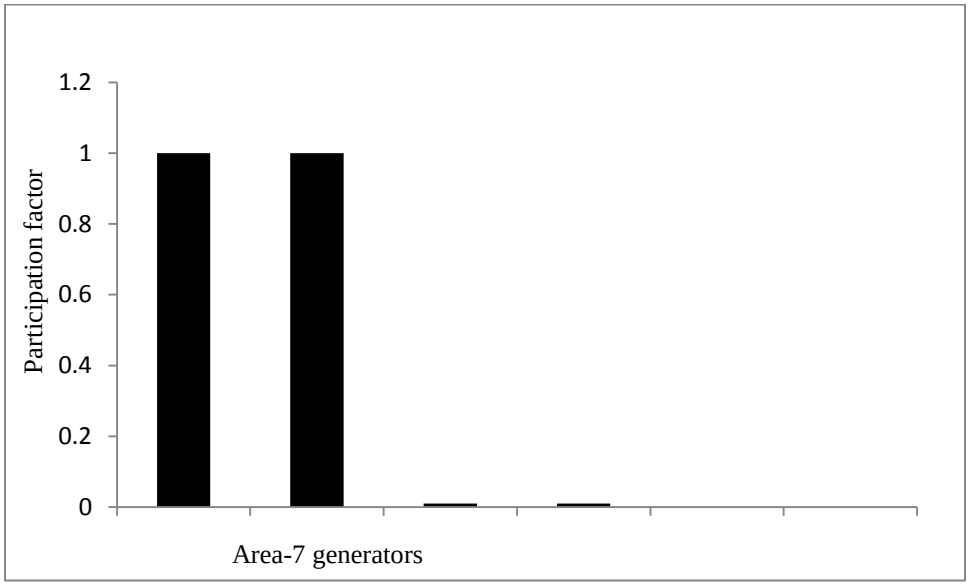

Figure 5.21 Participation factor corresponding to generator speed state for 0.4755 Hz inter-area mode in Max Wind case

Chapter 6. CONCLUSIONS AND FUTURE WORK

6.1 Conclusions

This thesis deals with the impact of reduced system inertia due to increased renewable penetration on power system transient stability and small-signal stability. In addition, the causes behind the research findings are investigated.

A detailed analysis of the Max Solar and Max Wind cases was performed by conducting static *N-1* and *N-2* contingencies. These results were then used as a guide to select cases for transient stability analysis.

Detailed transient stability analysis for *N-1* contingencies showed that no *N-1* contingency resulted in transient instability for any of the cases. Therefore, the impact of *N-2* contingencies was given attention.

The Max Wind case has one contingency which results in several generators losing synchronism. This is a local phenomenon and does not appear to have a system wide impact. An interesting feature of the Max Wind case is that a large disturbance which completely isolates the wind generation only causes two small local generators to lose synchronism and does not have a major impact on the system. The Max Solar case is found to be the more stressed case. There are three *N-2* contingencies which result in the loss of synchronism of several generators and tripping these generators does not stabilize the system.

The ability to reach a post-disturbance steady state following the loss of significant amounts of wind or solar generation was also investigated. Due to the inter-connected system configuration, loss of even the biggest wind or solar hubs is compensated without exceeding system generation and transmission limits.

Given the large penetration of wind and solar resources, analysis was also conducted to examine the impact of reduced reserve and the possibility of replacing CST plants by PV solar on system performance. Depending on the point of the renewable injection in the AC network and the amount of injection, faults with different locations and severity affect some of the remaining conventionally synchronous generators in an adverse fashion and some other conventional generators are affected favorably.

Further studies were performed to compare the performance of the two cases with the corresponding cases with no renewables. The magnitudes of initial steady state rotor angles were compared for the corresponding cases and explanations were provided for the difference in response to same disturbance on different cases.

Small signal stability studies were conducted to examine the most critical inter-area modes of oscillations corresponding to rotor speeds. These studies also confirm that the generators within the study area do not participate in the critical modes having low damping ratios.

It can be concluded that a suitably designed power system can accommodate high penetrations of wind and solar generations without compromising its transient and small-signal stability. Although some instability issues can arise, but they are due to very severe *N-2* contingencies.

6.2 Future work

In the present work, impact of renewables on system stability is discussed. This work can be extended by proposing some mitigation methods to correct the low damping problems associated with some inter-area modes of oscillations. In addition, the few severe instability problems could also be studied in more detail so as to provide corrective measures or protection to the rest of the system.

Since, wind and solar PV resources do not provide much reactive power support and because of phasing out of conventional synchronous machines, the system may require additional sources of reactive power. Additional analytical studies could be performed to investigate this aspect.

REFERENCES

[1] A. Best, “Transmission boost,” Planning, v. 76, pp. 24-28, Feb. 2010.

[2] U.S. Energy Information Administration, “Electric power monthly-March 2012,” http://www.eia.gov/cneaf/electricity/epm/epm_sum..html, March 2012.

[3] J.J. Grainger and W.D. Stevenson, “Power system analysis,” New York, McGraw-Hill, 1994.

[4] H. Knudsen and J.N. Nielsen, “Introduction to the modeling of wind turbines,” in Wind power in power systems, T. Ackermann, Ed. Chicester, U.K.: Wiley, 2005, pp. 525-585.

[5] E. Muljadi, C. Butterfield, B. Parsons and A. Ellis, "Effect of variable speed wind turbine generator on stability of a weak grid," IEEE Transactions on Energy Conversion, vol. 22, no. 1, pp. 29-36, 2007

[6] L. Holdsworth, X. G. Wu, J. B. Ekanayake and N. Jenkins, “Comparison of fixed speed and doubly-fed induction wind turbines during power system disturbances,” IEEE Generation, Transmission and Distribution, vol. 150, no. 3, pp. 343-352, 13 May 2003.

[7] G. Tsourakis, B. M. Nomikos and C. D. Vournas, “Contribution of doubly fed wind generators to oscillation damping,” IEEE Transactions on Energy Conversion, vol. 24, no. 3, pp. 783-791, September 2009.

[8] A. Mendonca and J. A. P. Lopes, “Impact of large scale wind power integration on small signal stability,” International conference on Future Power Systems, pp. 5, 18 November 2005.

[9] A. Mendonca and J. A. P. Lopes, “Simultaneous tuning of power system stabilizers installed in DFIG bases wind generation,” IEEE Lausanne Power Tech, pp. 219-224, 1-5 July 2007.

[10] F. M. Hughes, O. Anaya-Lara, N. Jenkins and G. Strbac, “A power system stabilizer for DFIG-based winf generation,” IEEE Transactions on Power Systems, vol. 21, no. 2, pp. 763-772, May 2006.

[11] D. Gautam, V. Vittal and T. Harbour, “Impact of increased penetration of DFIG-based wind turbine generations on transient and small signal stability of power systems,” IEEE Transactions on Power Systems, vol. 24, no. 3, pp. 1426-1434, August 2009.

[12] D. Gautam, V. Vittal and T. Harbour, "Supplementary control for damping power oscillations due to increased penetration of doubly fed induction generators in large power systems," IEEE/PES Power Systems Conference and Exposition, pp. 1-6, 20-23 March 2011.

[13] L. Meegahapola and D. Flynn, "Impact on transient and frequency stability for a power system at very high wind penetration," IEEE/Power and Energy Society General Meeting, pp. 1-8, 25-29 July 2010.

[14] B. Tamimi, C. Canizares and K. Bhattacharya, "Modeling and performance analysis of large solar photovoltaic generation on voltage stability and inter-area oscillations," IEEE/Power and Energy Society General Meeting, pp. 1-6, 24-29 July 2011.

[15] Liu Haifend, Jin Licheng, D. Le and A. A. Chowdhury, "Impact of high penetration of solar photovoltaic generation on power system small signal stability," International Conference on Power System Technology (POWERCON), pp. 1-7, 24-28 October 2010.

[16] W. Du, H. F. Wang and R. Dunn, "Power system small signal oscillation stability as affected by large-scale PV penetration," International Conference on Sustainable Power Generation and Supply, pp. 1-6, 6-7 April 2009.

[17] Yun Tiam Tan and D. S. Kirschen, "Impact on the power system of a large penetration of photovoltaic generation," IEEE/Power and Energy Society General Meeting, pp. 1-8, 24-28 June 2007.

[18] O.D. Mipoung, L.A.C. Lopes and P. Pillay, "Power estimation of induction generators fed from wind turbines," IEEE Industry Applications Society Meeting, pp. 1-6, 9-13 Oct 2011.

[19] CIGRE Technical Brochure, "Modeling and dynamic behavior of wind generation as it relates to power system control and dynamic performance," Working Group 01, Advisory Group 6, Study Committee C4, Draft Report, August 2006

[20] J. Usaola and P. Ledesma, "Dynamic incidence of wind turbines in networks with high wind penetration," Proc. 2001 IEEE Power Engineering Society Summer Meeting, pp. 755-760.

[21] GE Energy Technical Brochure, "Modeling of GE solar photovoltaic plants for grid studies", Version 1.1, April 16, 2010.

[22] GE Energy Technical Brochure, "Modeling of GE wind-turbine generators for grid studies", Version 1.1, April 16, 2010.

[23] P. Kundur, Power system stability and control, New York: McGraw Hill Inc., 1994.

[24] P.M. Anderson and A.A. Fouad, Power system control and stability, N.J.: John Wiley & Sons, Inc., 2002.

[25] F.M. Hughes, O.A. Lara, N. Jenkins and G. Strbac, "Control of DFIG-based wind generation for power network support," IEEE Transactions on Power Systems, vol. 23, no. 2, pp. 729-736, May 2008.

[26] General Electric Inc., PSLF model manual, Version 17.0_05.

[27] Powertech Labs Inc., DSA Tools model manual, Version 11.0.